Supplemental Materials and Methods

All the antibodies, reagents, cell lines, constructs and softwares are shown in Supplemental Table 8.

Human iPSC generation

For lentivirus-based hiPSC generation, cells were transduced with lentiviral particles from individual lentiviral vectors or polycistronic STEMCCA vectors containing Y4 factors (OCT4, SOX2, KLF4, and C-MYC; generously provided by Dr. Gustavo Mostoslavsky) and/or miRNAs overnight. Next day, the medium was exchanged with induction medium and cells incubated for 5 days. On day 6, cells were fed with hiPSC medium and kept in that medium until formation of ES-like colonies. The observed ESC-like colonies were handpicked and transferred onto Matrigel-coated tissue culture plates in Essential 8 medium to generate hiPSC lines.

For episomal system-based hiPSC generation, cells were electroporated with reprogramming factors-expressing pCXLE vector using the Neon transfection system, then plated onto a Matrigel-coated, 6 well plate in hDF medium supplemented with 10 μM Y-27632. Next day, cells were fed with Induction medium for additional 5 days.

Plasmid construction and lentivirus production

Coding sequences for individual miRNAs for miR-17/92, -106a, -106b, -200c, -302s, -369s and -371/373 were PCR-amplified from H9 hESCs, cloned into the pGEM-T Easy vector and their identify confirmed by sequencing. Subsequently, they were introduced into the EcoRI site of the FUW-tetO vector. For the OCT4, KLF4, SOX2, and L-MYC-expressing polycistronic episomal vector, human Oct4 linked with 2A sequence of foot-and-mouth disease virus (OCT4-F2A), KLF4, SOX2 linked with 2A sequence of porcine teschovirus (SOX2-P2A), and L-MYC coding sequences were PCR-amplified from H9 hESCs, then introduced sequentially into a modified pCXLE episomal vector freed of EGFP sequences. For miR-302s and/or miR-200c expressing episomal vector, human miR-302s or -200c coding sequences were introduced into the modified pCXLE vector.

Lentivirus production was performed as described previously with slight modifications (1). Briefly, lentiviral vectors were co-transfected with packaging plasmids including pMD2.G, and psPAX2 into 293T cells, maintained in DMEM supplemented with 10% FBS, using PolyJet transfection reagent according to the manufacturer's instruction. Supernatants containing lentiviruses were collected 48 h post-transfection and filtered through 0.45 μm Millex-HV (Millipore) filters to remove cell debris.

hiPSC formation assay

For TRA-1-60 staining, cells were fixed with 4% formaldehyde for 5 min, washed with PBS and then incubated with anti-TRA-1-60 antibody (1:500) at 4℃ overnight. After three washes with PBS cells were incubated for 1 h with horseradish peroxidase (HRP)-conjugated goat anti-mouse IgG (1:500). After washing three times with 0.1% Triton X-100 in PBS, cells were stained with 3,3'-diaminobenzidine (DAB) following the manufacturer's instructions. For AP staining, fixed cells were washed with PBS and then stained with a solution of the alkaline phosphatase substrate NBT/BCIP followed by three washes with PBS to stop the reaction.

Live cell metabolic analysis

Oxygen consumption rate (OCR) and extracellular acidification rate (ECAR) were measured using the XFp analyzer (Agilent Technologies) according to the manufacturer's instruction. Briefly, cells were plated onto wells of an XF mini-plate and incubated at 37°C in a CO_2 incubator overnight. The assay was performed after cells were equilibrated for 1 h in XF assay medium supplemented with 10 mM glucose, 5 mM sodium pyruvate, and 2 mM L-glutamine in a non-CO_2 incubator. hDFs' mitochondrial activity was monitored through sequential injections of 1 μM oligomycin (Oligo), 2

μM FCCP, and 0.5 μM antimycin A/rotenone (Anti/Rot) to calculate basal respiration (= baseline OCR - Anti/Rot OCR), ATP turnover (= basal respiration - Oligo OCR), maximum respiration (= FCCP OCR - Anti/Rot OCR), and oxidative reserve (= maximum respiration - basal respiration). Each plotted value was normalized to total protein quantified using the Bradford protein assay.

Quantitative RT-PCR

To extract total RNA, cells were lysed with Trizol and RNA was separated according to the manufacturer's recommendations. RNA concentration was measured using a Nanodrop ND-1000 spectrophotometer (NanoDrop Technologies). RNAs were reverse transcribed with oligo dT primer using Superscript II. For real time quantitative RT-PCR we used SsoAdvanced Universal SYBR Green Supermix and reactions were performed on a CFX Connect Real-Time System (Bio-Rad). PCR amplification was performed using gene-specific primers (Supplemental Table 7). Target gene expression was determined by normalization to endogenous ACTIN by the comparative cycle time method.

Karyotype analysis

To evaluate the number and structure of the human iPS cells chromosomes, human iPS cells were sent to Cell Line Genetics, Inc (Madison, WI) for standard G-banded karyotype analyses.

Episomal plasmid detection

Cytosolic plasmids were obtained using the Thermo Scientific GeneJET Plasmid Miniprep Kit to detect the presence of residual non-integrated vector. For each 20 μl of plasmid extract, 2 μl were amplified using the profile 95°C 30 sec, 55°C 30 sec and 72°C 30 sec for 30 cycles with EBNA specific primers. Genomic DNA was prepared with Qiagen's DNeasy Blood & Tissue Kit. For detection of plasmid derived sequences, we used same PCR amplification conditions described above and EBNA primers. There were five EBNA specific primers been tested. GAPDH primers were used as input control. All the EBNA and GAPDH primer sequences present in Supplemental Table 7.

DNA fingerprinting

Genomic DNA was extracted using the QIAamp DNA FFPE Tissue Kit and PCR performed using standard buffer conditions, 0.2 μg of DNA and GoTaq DNA polymerase and 35 cycles of the following amplification protocol: 95°C for 30 sec, annealing at 55°C for 30 sec, and extension at 72°C for 1 min in a total volume of 20 μl. Primers used in this study are listed in Supplemental Table 7.

Whole exome sequencing

To identify somatic mutations resulting from fibroblasts reprogramming and passaging of reprogrammed iPSCs, we performed WES of fibroblast and of four iPSC lines using the Personalis ACE WES service providing augmented coverage of >8,000 medically implicated genes, including >1,400 cancer-related genes (2). Mean depth of coverage for target regions was over 75x across all samples. For the four iPSC lines, we performed paired analysis of fibroblast and each iPSC line to detect somatic mutations using MuTect2 (3).

Sequencing reads were aligned to GRCh38 reference genome including alternative contigs and decoys using the BWA-MEM program (version 0.7.15) (4). The mapped reads were further processed with SAMtools (version 1.3.1) (5), Picard tools (http://broadinstitute.github.io/picard, version 2.5.0) and Genome Analysis Tool Kit (GATK) software (version 3.6) (6) to generate analysis-ready BAM files. Each iPSC line was analyzed for somatic mutations compared to fibroblasts using the MuTect2 module in GATK (3). Identified somatic mutations were annotated using the Ensembl Variant Effect Predictor (version GRCh38.89) (7) to investigate their

consequences on gene transcription and protein product. To reduce false positive somatic mutation calls, we only considered those discovered in well covered regions with 20 or more effective high-quality aligned reads across all samples. Among the candidates, we excluded mutations with maximum minor allele frequency > 0.01% in the Exome Aggregation Consortium (ExAC) database (8) to filter out potential germline variants. For the remaining somatic mutation candidates, we queried the Catalogue Of Somatic Mutations In Cancer (COSMIC) (http://cancer.sanger.ac.uk, version 80) (9) and Cancer Gene Census (CGC) databases (10) to identify frequently reported mutations and genes in cancer. We investigated chromosomal aberrations and other regional changes in copy number using ngCGH (https://github.com/seandavi/ngCGH, version 0.4.4) and copy number variation (CNV) analysis results from the Personalis ACE Cancer Exome pipeline (Personalis, Inc., CA). We visually inspected all CNV candidates for read alignments in Integrated Genome Viewer (version 2.3.79).

Quercetin treatment

To test the effect of Quercetin on human iPSC removal, human iPSCs were plated on 6 well plates. Cells were treated with each concentration of Quercetin (5, 10, 20, 40, and 100 µM) for 2, 6, 16, and 24 hours. After each time point, Quercetin containing medium was replaced with fresh medium and cells cultured for 48 hours from the initial Quercetin treatment time. Cells were dissociated using TrypLE and cell viability was measured using Trypan blue exclusion and hemocytometer.

Flow cytometry

All the FACS analysis were performed using BD Accuri C6 system (BD Bioscience) and data analyses were carried out according to manufacturer's instructions. Human iPS Cells were dissociated using TrypLE or Accutase, respectively, and filtered through a 70 µm cell strainer. Single cell suspensions were first fixed with 4 % formaldehyde for 10 mins and suspended in permeabilization buffer for 15 min on ice. After blocking for 30 min, cells were incubated with primary labeled antibodies (PE conjugated anti SSEA-4, TRA-1-60) for 1 hour on ice in the dark. After washing with PBS with 1% FBS, FACS analysis was performed. Fluorochrome matched isotype controls were used and subtracted during analysis.

For cell loss/cell harvest analysis, the supernatant from monolayer- or spotting- based culture dish were harvested and run FACS. The particle numbers in 100 µl of supernatant were calculated and the total cell numbers were obtained based on the ratio of 100 µl to total supernatant volume.

Detecting the presence of undifferentiated cells

Mixtures of undifferentiated C4 cells were serially diluted among hDFs by successive factors of 10 (10^5, 10^4, 10^3, 10^2, 10^1 and 10^0) in a total of 100,000 cells to detect residual C4 cells using 3 different methods. For colony forming assay, each cell dilution was cultured for 6 days in E8 medium and pluripotent colonies were identified by AP staining. For the quercetin removal of undifferentiated cells, cells were treated with 40 µM quercetin for 16 hours and cultured in fresh E8 medium. For fluorescence activated cell sorting (FACS), C4 cells were dissociated using TrypLE and filtered through a 70 µm cell strainer. Single cell suspensions were first fixed with 4% formaldehyde for 10 mins and suspended in permeabilization buffer for 15 min on ice. After blocking for 30 min, cells were incubated with primary labeled antibodies (PE conjugated anti SSEA-4, TRA-1-60) for 1 hour on ice in the dark. After washing with PBS with 1% FBS, FACS analysis was performed using a BD Accuri C6 system (BD Bioscience) and data analyses were carried out according to manufacturer's instructions. Fluorochrome matched isotype controls were used and subtracted during analysis. For qRT-PCR assay, total RNA from all dilutions was extracted and subjected to qRT-PCR to determine OCT4 cycle times (Ct) value. OCT4 copy

numbers were calculated from the equation curve that was generated from qRT-PCR of purified OCT4 partial sequence. Then, OCT4 copy numbers were plotted against PSC numbers.

Spotted Dish Preparation

As shown in Figure S3B, a grid consisting of 2 horizontal and 3 vertical lines was drawn at the bottom of 6-cm dishes yielding 6 junctions. 10 µl of cold Matrigel was loaded at each junction to make a limited spot-coated area. The spotted dishes were incubated at 37^{o}C for at least 30 min and the Matrigel was aspirated just before cell plating. Homogenously suspended cells were plated at a density of 730K/dish in 60mm cell culture dish (regular plating conditions) while the spotted dishes received either 40K/10 µl spot, 10K/10 µl spot, 2.5K/10 µl spot (spotting conditions).

mDA Progenitor Differentiation

Differentiation media conditions and all the morphogen factors are shown in Figure 5A. Through the entire differentiation procedure, no antibiotics were used. For the floor plate induction stage (D1-6), we used DMEM media with 15% KSR, glutamine, β-mercaptoethanol. For the neural precursor induction stage (D6-12), we used DMEM media with 11.5 % KSR, 0.25% N2 (D6-8), 7.5 % KSR, 0.5% N2 (D8-10), 3.75 % KSR, 0.75% N2 (D10-12) including L-glutamine, β-mercaptoethanol and non-essential amino acid (NEAA). Dual Smad inhibitors, 0.2 µM LDN193189 and 10 µM SB431542 were added from D1-D12, and D1-D8, respectively. From D2 to D10, cells were treated with SHH agonist (2 µM Purmorphamine and 100 ng/ml Shh) with 100 ng/ml FGF8. The Wnt signaling activator, CHIR99021 (1 µM), was included from D4 to D12. At D9, cells were treated with 40 µM quercetin for 16 hours. For the DA progenitor induction and maturation stage (D12+), DMEM:F12 media was supplemented with N2 supplement, 20 ng/ml BDNF, 20 ng/ml GDNF, 500µM dbcAMP, 200 µM ascorbic acid, 10 ng/ml TGF-β3, along with 10µM DAPT and 1µM CHIR (D12-15). At D15, the cells were dissociated by 0.5mM EDTA and the single cell suspension were re-plated in Poly-L-ornithine/Fibronectin/Laminin-coated dishes at approximately 2.5 millions/dish. From D15 onward, DMEM:F12 media was applied with N2 supplement, 20 ng/ml BDNF, 20 ng/ml GDNF, 500 µM dbcAMP, 200 µM ascorbic acid, 10 ng/ml TGF-β3. At harvest, 10 µM Y-27632 was added to the medium.

Immunocytochemistry

hiPSC derived dopaminergic neurons were washed with phosphate-buffered saline (PBS) (with Ca^{2+} and Mg^{2+}) and fixed with 4% formaldehyde in PBS (pH 7.4) for 10 mins. Cells were incubated for 1 hr in blocking solution (0.3% Triton X-100 and 1% horse serum in PBS) at room temperature. Cells were incubated with primary antibodies in PBS containing 0.3% Triton X-100 and 1% horse serum overnight. Cells were then incubated with the proper fluorescence-conjugated secondary antibodies with Hoechst 33342 for nuclei staining at room temperature for 1 hr. Cell images were obtained by confocal microscopy (KEYENCE, Osaka, Japan). Data regarding specific cell populations were determined from microscopic images using ImageJ software (11). To measure apoptotic cells, cells were stained for cleaved caspase 3, an apoptotic marker, and Hoechst 33342, a DNA-binding nuclear dye. After staining with Hoechst 33342, compacted chromatin is brighter than in normal cells, and the condensed nuclei were counted by fluorescence microscopy. Data regarding specific cell populations were determined from microscopic images by ImageJ software.

High-performance liquid chromatography (HPLC) analysis

On day 47 of differentiation, supernatants were collected and centrifuged at 300 x g for 5 min to remove cell debris. Samples were immediately stored at −80°C and shipped to Emory University's HPLC Bioanalytical Core for reverse phase HPLC with electrochemical detection to determine the levels of DA and DOPAC. In brief, the supernatants were transferred into fresh 0.22 µM PVDF microcentrifuge filtered tubes. Any remaining particulate matter was eliminated by filtration

through the spin filter at 5000 rpm for 5 min at 4ºC. Monoamine concentrations were determined by reverse phase HPLC with electrochemical detection. For HPLC, an ESA 5600A CoulArray detection system, equipped with an ESA Model 584 pump and an ESA 542 refrigerated autosampler was used. Separations were performed at 25ºC using an MD-150 × 3.2 mm C18 column equipped with a C18 column guard cartridge. The mobile phase consisted of 1.5 mM 1-octanesulfonic acid sodium, 75 mM NaH2PO4, 0.025% triethylamine, and 8% acetonitrile at pH 2.95. Sample volumes of 25 µl were injected. Samples were eluted isocratically at 0.4 mL/min and detected using a 6210 electrochemical cell (ESA, Bedford, MA) equipped with a 5020 guard cell. The Guard cell potential was set at 500 mV, while analytical cell potentials were −175, 200, 350 and 425 mV. The analytes were identified by the matching criteria of retention time to known standards (Sigma Chemical Co., St. Louis MO). Compounds were quantified by comparing peak areas to those of standards on the dominant sensor.

Electrophysiology

For electrophysiological recordings, day 70 dopaminergic cells were placed in the recording chamber and continuously perfused at the rate of 1.2 ml/min with artificial cerebrospinal fluid consisting of 130 mM NaCl, 2.5 mM KCl, 2.5 mM $CaCl_2$, 1 mM $MgSO_4$, 1.25 mM Na_2HPO4, 26 mM $NaHCO_3$, 10 mM glucose, which was continuously bubbled with 95% O_2 and 5% CO_2. Whole-cell patch-clamp recordings were performed at room temperature (22 ± 1.0 °C) using a EPC9 amplifier and Pulse v8.80 software (HEKA Elektronik). The recording electrodes (5-6 MΩ resistance) were filled with pipette solution containing 150 mM K-gluconate, 5 mM NaCl, 1 mM $MgCl_2$, 0.2 mM EGTA, 10 mM HEPES, 2 mM Mg-ATP, 0.5 mM Na-GTP (292 mOsm, adjusted to pH 7.3 with KOH). The liquid junction potential of 15.1 mV was corrected for using K-gluconate-based pipette solution. In current clamping mode, action potential firing was recorded at the resting membrane potential. Series (access) resistance was not compensated but continuously monitored. Spontaneous synaptic events were analyzed offline using Mini Analysis v6.0.7 (Synaptosoft) and Clampfit 8.2 (Molecular Devices) programs. Voltage-gated sodium channels were blocked with 1 µM Tetrodotoxin (TTX). Neurobiotin (0.2 %) was included in intrapipette solution and recorded cells were fixed in 4% formaldehyde at 4°C and co-stained with TH antibody.

Multi-electrode array (MEA) recording

24-well microelectrode array (MEA) plate from Axion Biosystems were precoated with Poly L-ornithine (0.0015%), Fibronectin (1 µg/ml) and Laminin (1 µg/ml) for one night each at 37°C in a CO_2 incubator. Next day, C4 derived D28 cells were plated at 20,000/well on the pre-coated MEA plate and generated according to the same schedule as described above. D28 cells were maintained in a humidified incubator at 37°C with 5% CO_2 for 2 days to allow for proper attachment before electrophysiological recordings were initiated. A 60% medium change was performed every other day. Extracellular recordings of spontaneous action potentials were performed in culture medium at 37°C using a Maestro MEA system and AxIS software (Axion Biosystems before and after treatment with compounds. This MEA platform is configured with 324 channels, and when using 24-well plates, is formatted to have 16 electrodes per well in a 4 × 4 grid. Approximately 20,000 cells were plated in each well dotted on the electrode grid. The baseline and post treatment raw data files (*.raw) were converted to spike files (*.spk) and excel files (*.csv) using AxIS Navigator 1.5.1 software. The conversion to these file formats allows for further processing and analysis of the data. For mDA neurons, the measurement for neural spikes within the AxIS software was set with a high pass = 200 Hz and a low pass = 3,000 Hz. The threshold for spike detection was set to 6 times the rolling standard deviation of the filtered field potential on each electrode. Five-minute recordings were used to calculate the average spike rate and the number of active electrodes in each well (“Active Electrodes”). An active electrode was defined as an electrode with a spike rate ≥ 5spks/min.

Axion BioSystems' Neural Metric Tool was used to inspect the spike train raster plots to verify both the robustness of the activity and the quality and consistency of the well activity. These raster plot visualizations were also used to assist in the interpretation of the post treatment data. Wells with no spike activity, sparse spike activity, or little or no bursting or network synchrony are excluded from the experiment. Plates were equilibrated on the system for at least 2 min before the recording commences. In order to isolate dopaminergic neurons spontaneous activity, cells were treated with a combination of picrotoxin, a GABAergic antagonist; NBQX, an AMPA receptor antagonist; and AP5 NMDAR antagonist, all at a concentration of 10 µM in 500 µl of media per well. After adding the blocker, both the average number of spikes and the average number of electrodes was calculated. Recordings and analysis were done as mentioned above. A t-test was used to compare the average number of spikes and the average number of active electrodes between the control and treated groups.

Cell preparation for Transplantation and Cryopreservation

C4-derived D28 cells were rinsed twice with DPBS and then treated with Accutase for 5 min at 37°C. Cells were harvested using DMEM:F12 medium with N2 supplement, 20 ng/ml BDNF, 20 ng/ml GDNF, 500 µM dbcAMP, 200 µM ascorbic acid, 10 ng/ml TGF-β3, and 10 µM Y-27632). After centrifugation at 300 x g for 3 mins, cell pellets were suspended with transplantation medium (DMEM/F-12 (without phenol red), 20 ng/ml BDNF, 20 ng/ml GDNF, 10 µM Y-27632, 20 mM Boc-D-FMK). Cell suspensions were passed through a 70 µm strainer to remove big clumps. Cell concentrations were calculated by Trypan blue exclusion using a hemocytometer. The final cell product consisted of 50,000 or 100,000 cells/µl in transplantation medium. For cryopreservation, cell pellets were suspended in CryoStor® CS10 cryopreservation medium. Cells in cryovials were placed into a Mr. Frosty™ Freezing Container (Nalgene) for controlled freezing at -80ºC. Frozen cells were then transferred to liquid nitrogen. After one week, frozen cells were thawed for transplantation.

Surgical Procedure

Animals were anesthetized with isoflurane using a SomnoSuite Anesthesia System (Kent Scientific Corporation, Torrington, CT). Stereotaxic surgeries were performed on a stereotaxic frame (David KOPF Instruments, Tujunga, CA) equipped with a Micro4 controller (World Precision Instruments, Sarasota, FL).

For Charles River athymic rats, unilateral lesions of the nigrostriatal pathway were established by stereotaxic injection of 6-OHDA into the medial forebrain bundle. Desipramine (10 mg/kg) was injected into the rats to protect noradrenergic projections 15 min prior to anesthesia. Two microliters of 6-OHDA (7.5 mg/ml in 0.2% ascorbic acid and 0.9% saline) were injected using a 2.5 µl Hamilton syringe (Hamilton Company, Reno, NV). The coordinates were calculated with reference to bregma: antero-posterior (AP), -4.0; medio-lateral (ML), -1.3; and dorsoventral (DV), -7.0 (12). For intra-striatal transplantation of H9 or C4-derived D28 cells, one deposit of 2 µl (50,000 cells/µl) was placed at the following coordinates: AP, +0.8; ML, -3.0; and DV, -5.5. Cells were injected through a 10 µl Hamilton syringe fitted with a blunt 26G, 0.75-inch needle at a speed of 0.4 µl/min. For Taconic athymic rats, C4 D28 cells were suspended at a concentration of 100,000 cells/µl. One microliter of cells was injected into AP, +0.8; ML, -3.0; and DV, -5.5 for the 100,000 cell group. For the 300,000 cell group, two deposits of 1.5 µl were placed at the following coordinates: AP, +0.8; ML, -3.0; and DV, -5.0 and DV, -6.0. Control rats only received transplantation medium injections. For NOD SCID mouse striatal injections, one deposit of 2 µl (50,000 cells/µl) of C4 Do, D14 or D28 cells were injected in the striatum, according to the following co-ordinates relative to bregma (in mm): AP +0.5; ML -/+1.8; DV -3.2 bilaterally.

After injection, the needle was kept in the brain for 5 min. and then the needle was withdrawn slowly over a period of 5 min. After surgery, the incised skin was sealed with Autoclip® Surgical

Suture (Fine science tools, Foster City, CA) and animals were monitored on a warm pad until recovery. All animals were injected with Ketoprofen (5mg/kg; Ketofen, Santa Cruz, SC-363115Rx) subcutaneously to reduce pain and 1ml 0.9% sodium chloride intraperitoneally to prevent dehydration.
For NOD SCID mouse testis injection, a 1 cm longitudinal incision was made through the skin and peritoneum, and the testes placed on sterile gauze. 10 µl (5,000/µl) of C4 iPSC were slowly injected into the center of the testis capsule away from any major blood vessels. The needle was removed slowly to avoid reflux of the cells. The testes and fatty tissue were replaced back to their original position in the abdomen.

D-Amphetamine-induced rotation test
D-Amphetamine, a presynaptic (indirect) DA agonist, was administrated intraperitoneally (4 mg/kg) to induce rotational behavior in rats that have been successfully lesioned with 6-OHDA. Rotational bias was recorded using an automated system (SD Instruments, San Diego, CA). Rats were recorded for 90 min (9 intervals; 10 min/interval). Only full body turns were counted and then expressed as net turns per minute, with rotations toward the side of the lesion given a positive value. Only animals showing more than 6 ipsilateral turns per minute were considered successfully lesioned (13).

Corridor test
To measure non-pharmacological behavior improvement, we used the corridor test (14). First, to reduce exploratory behavior during testing, rats were habituated to the corridor with scattered sugar pellets for 10 min for 2 days. The next day, rats were placed at the end of a corridor with 10 adjacent pairs of cups filled with 5-10 sugar pellets consistently distanced along the floor of the corridor. Animals were allowed to explore the corridor freely. An investigator blinded to the group identity directly counted retrievals. A ‘retrieval’ was defined as each time the rat poked its nose into a unique cup. All rats were tested until 20 retrievals were made or the test duration reached 5 minutes. Before testing, all rats were located in an empty corridor for 5 minutes to reduce environment novelty. Rats were food restricted the day prior and during the 4 days of testing. Results were calculated as an average of the contralateral retrievals (right) and presented as percentage of total retrievals. Tests were performed every 4 weeks until 24 weeks after transplantation.

Cylinder test
To measure forelimb asymmetry in exploratory behavior, rats were assessed using the cylinder task (15), where the rat is placed in a glass cylinder (20 cm in diameter) and a maximum of 30 paw touches to the walls are recorded. An investigator blinded to the group identity made the evaluation. Results were calculated as an average of touches using the right-side paw (contralateral) and presented as percentage of average of total touches. Tests were performed 24 weeks after transplantation.

Stepping test
To measure forelimb akinesia, rats were assessed using the side-stepping test (16), where forelimb adjusting steps are quantified over a total length of 90 cm. Steps were counted by an investigator blinded to the group identity. Results were calculated as an average of the number of right forelimb steps (contralateral) and presented as percentage of average of the left forelimb steps. Tests were performed 24 weeks after transplantation.

Bio-distribution Analysis

To verify the existence of transplanted human cells we used RT-PCR method specific for amplification of human specific gene. First DNA was extracted from each 15mg of mouse tissue (olfactory bulb and cerebellum mixture, spinal cord, lung, heart, liver, kidney, and spleen) with QIAamp DNA FFPE Tissue Kit according to the manufacturer's instructions. The concentration of extracted DNA was measured on a Nanodrop ND-1000 spectrophotometer and 100ng of DNA was used for real time RT-PCR reaction. We used the following human specific primer sequences: forward 5'-ATTGCCCCAAAACTTTTTTG-3' and reverse 5'- TTGAAGACCAGTCTGGGAAG-3'. Endogenous mouse DNA was detected using the following primers: forward 5'-CCACATCTCCCTCCAGAAAA-3' and reverse 5'-AGGGTCTGGGCCATAGAACT-3'.

Brain Sectioning and Immunohistochemistry

Deep anesthesia was induced with an intraperitoneal injection of Ketamine (75 mg/kg)/Xylazine (7.5 mg/kg), followed by intracardial perfusion with ice-cold phosphate buffered saline (PBS; 0.01M, pH 7.4) for 8 min, followed by perfusion with 4% formaldehyde for 20 min, at a flow rate of 10 ml/min. Brains were removed and post-fixed overnight in 4% formaldehyde at 4 °C and then cryopreserved by successive incubations in 20% and 30% sucrose. Brains were embedded in OCT and coronal sections (30 µm) covering the entire striatum were serially collected (Leica CM1950, Buffalo Grove, IL). Brain slices were incubated with PBS containing 30% H_2O_2 for 30min and then were incubated with rabbit anti-TH antibody (1:5000), mouse anti-hNCAM antibody (1:1000) and mouse anti-hNuc (1:1000) overnight. After rinsing, the samples were stained with biotinylated secondary antibody (Vector Labs) for 1h. Finally, sections were visualized with the Vectastain Elite ABC kit and the DAB peroxidase substrate kit following the manufacturer's protocol. To count TH^+ neurons in the grafts, the optical fractionator probe of the Stereo Investigator (MBF Bioscience, Williston, VT) was used under 63X oil lens with counting frame 50 x 50 µm and grid size 200 x 200 µm. Final counts were corrected for series number (1:6) to get an estimate of the total number of TH positive neurons per animal brain.

Vimentin immunohistochemistry was performed by the Rodent Histopathology Core at Harvard Medical School, Boston, MA.

Brain sections Immunofluorescence

Free-floating coronal sections of the entire midbrain were pre-incubated in blocking solution containing 5% normal donkey serum, 3% BSA and 0.3% Triton X-100 in PBS at room temperature for 1 h. Primary antibodies were diluted in 3% BSA and 0.3% Triton X-100 in PBS and were applied overnight at 4 °C. After three washes with PBS containing 0.3% Tween 20, the sections were incubated with Alexa 488-, Alexa 568- or Alexa 647-conjugated secondary antibodies diluted in the same buffer as the primary antibodies for 1 hr at room temperature. All sections were counterstained with Hoechst 33342. Following three additional washes, a cover slip was applied over the sections with mounting media and visualized with a fluorescence microscope (KEYENCE, Osaka, Japan). Sections stained with secondary antibodies alone were processed and photographed under the same conditions and used as negative controls.

Hematoxylin and Eosin staining

For pathological analysis of NOD SCID mouse testes, each mouse was anesthetized by Ketamine/Xylazine and testes were removed and stored temporarily in 4% formaldehyde. For NOD SCID mouse brain tissue pathological analysis, every sixth coronal sections covering the entire striatum were mounted on a glass slide. Glass slides of testes and brain tissues were sent to the Rodent Histopathology Core at Harvard Medical School, Boston, MA for Hematoxylin and Eosin staining.

Quantification and Statistical Analysis

All experiments were performed in biological triplicate unless otherwise indicated. The exact number of samples (*n*) and the statistical tests used for each figure panel can be found in the figure legends. Statistical analyses were performed using the GraphPad Prism v7 software. A value of $p < 0.05$ was considered to be statistically significant. Throughout the figures, asterisks indicate the significance of the p value: *$p < 0.05$; **$p < 0.01$; ***$p < 0.001$. For the test of mutations present in fraction of cells within each iPSC line, p-values were generated by two-sided binomial test and adjusted by Bonferroni correction. The mutation data were analyzed and visualized using R.

Study Approval

Animal studies were performed in accordance with current National Institutes of Health guidelines and McLean Hospital/Harvard University Institutional Animal Care and Use Committee protocols (2015N000001 and 2015N000002). Skin biopsies from three healthy subjects and one sporadic PD patient (Supplemental Table 2) were taken with written informed consent under an IRB approved protocol (Partners IRB #2010P001100).

References:

1. Cha, Y., Han, M.J., Cha, H.J., Zoldan, J., Burkart, A., Jung, J.H., Jang, Y., Kim, C.H., Jeong, H.C., Kim, B.G., et al. 2017. Metabolic control of primed human pluripotent stem cell fate and function by the miR-200c-SIRT2 axis. *Nat Cell Biol* 19:445-456.
2. Patwardhan, A., Harris, J., Leng, N., Bartha, G., Church, D.M., Luo, S., Haudenschild, C., Pratt, M., Zook, J., Salit, M., et al. 2015. Achieving high-sensitivity for clinical applications using augmented exome sequencing. *Genome Med* 7:71.
3. Cibulskis, K., Lawrence, M.S., Carter, S.L., Sivachenko, A., Jaffe, D., Sougnez, C., Gabriel, S., Meyerson, M., Lander, E.S., and Getz, G. 2013. Sensitive detection of somatic point mutations in impure and heterogeneous cancer samples. *Nat Biotechnol* 31:213-219.
4. Li, H., and Durbin, R. 2010. Fast and accurate long-read alignment with Burrows-Wheeler transform. *Bioinformatics* 26:589-595.
5. Li, H., Handsaker, B., Wysoker, A., Fennell, T., Ruan, J., Homer, N., Marth, G., Abecasis, G., Durbin, R., and Genome Project Data Processing, S. 2009. The Sequence Alignment/Map format and SAMtools. *Bioinformatics* 25:2078-2079.
6. DePristo, M.A., Banks, E., Poplin, R., Garimella, K.V., Maguire, J.R., Hartl, C., Philippakis, A.A., del Angel, G., Rivas, M.A., Hanna, M., et al. 2011. A framework for variation discovery and genotyping using next-generation DNA sequencing data. *Nat Genet* 43:491-498.
7. McLaren, W., Gil, L., Hunt, S.E., Riat, H.S., Ritchie, G.R., Thormann, A., Flicek, P., and Cunningham, F. 2016. The Ensembl Variant Effect Predictor. *Genome Biol* 17:122.
8. Lek, M., Karczewski, K.J., Minikel, E.V., Samocha, K.E., Banks, E., Fennell, T., O'Donnell-Luria, A.H., Ware, J.S., Hill, A.J., Cummings, B.B., et al. 2016. Analysis of protein-coding genetic variation in 60,706 humans. *Nature* 536:285-291.
9. Forbes, S.A., Beare, D., Boutselakis, H., Bamford, S., Bindal, N., Tate, J., Cole, C.G., Ward, S., Dawson, E., Ponting, L., et al. 2017. COSMIC: somatic cancer genetics at high-resolution. *Nucleic Acids Res* 45:D777-D783.
10. Futreal, P.A., Coin, L., Marshall, M., Down, T., Hubbard, T., Wooster, R., Rahman, N., and Stratton, M.R. 2004. A census of human cancer genes. *Nat Rev Cancer* 4:177-183.

11. Jeon, J., Kim, W., Jang, J., Isacson, O., and Seo, H. 2016. Gene therapy by proteasome activator, PA28gamma, improves motor coordination and proteasome function in Huntington's disease YAC128 mice. *Neuroscience* 324:20-28.
12. Torres, E.M., Lane, E.L., Heuer, A., Smith, G.A., Murphy, E., and Dunnett, S.B. 2011. Increased efficacy of the 6-hydroxydopamine lesion of the median forebrain bundle in small rats, by modification of the stereotaxic coordinates. *J Neurosci Methods* 200:29-35.
13. Kirkeby, A., Grealish, S., Wolf, D.A., Nelander, J., Wood, J., Lundblad, M., Lindvall, O., and Parmar, M. 2012. Generation of regionally specified neural progenitors and functional neurons from human embryonic stem cells under defined conditions. *Cell Rep* 1:703-714.
14. Dowd, E., Monville, C., Torres, E.M., and Dunnett, S.B. 2005. The Corridor Task: a simple test of lateralised response selection sensitive to unilateral dopamine deafferentation and graft-derived dopamine replacement in the striatum. *Brain Res Bull* 68:24-30.
15. Bjorklund, T., Carlsson, T., Cederfjall, E.A., Carta, M., and Kirik, D. 2010. Optimized adeno-associated viral vector-mediated striatal DOPA delivery restores sensorimotor function and prevents dyskinesias in a model of advanced Parkinson's disease. *Brain* 133:496-511.
16. Olsson, M., Nikkhah, G., Bentlage, C., and Bjorklund, A. 1995. Forelimb akinesia in the rat Parkinson model: differential effects of dopamine agonists and nigral transplants as assessed by a new stepping test. *J Neurosci* 15:3863-3875.

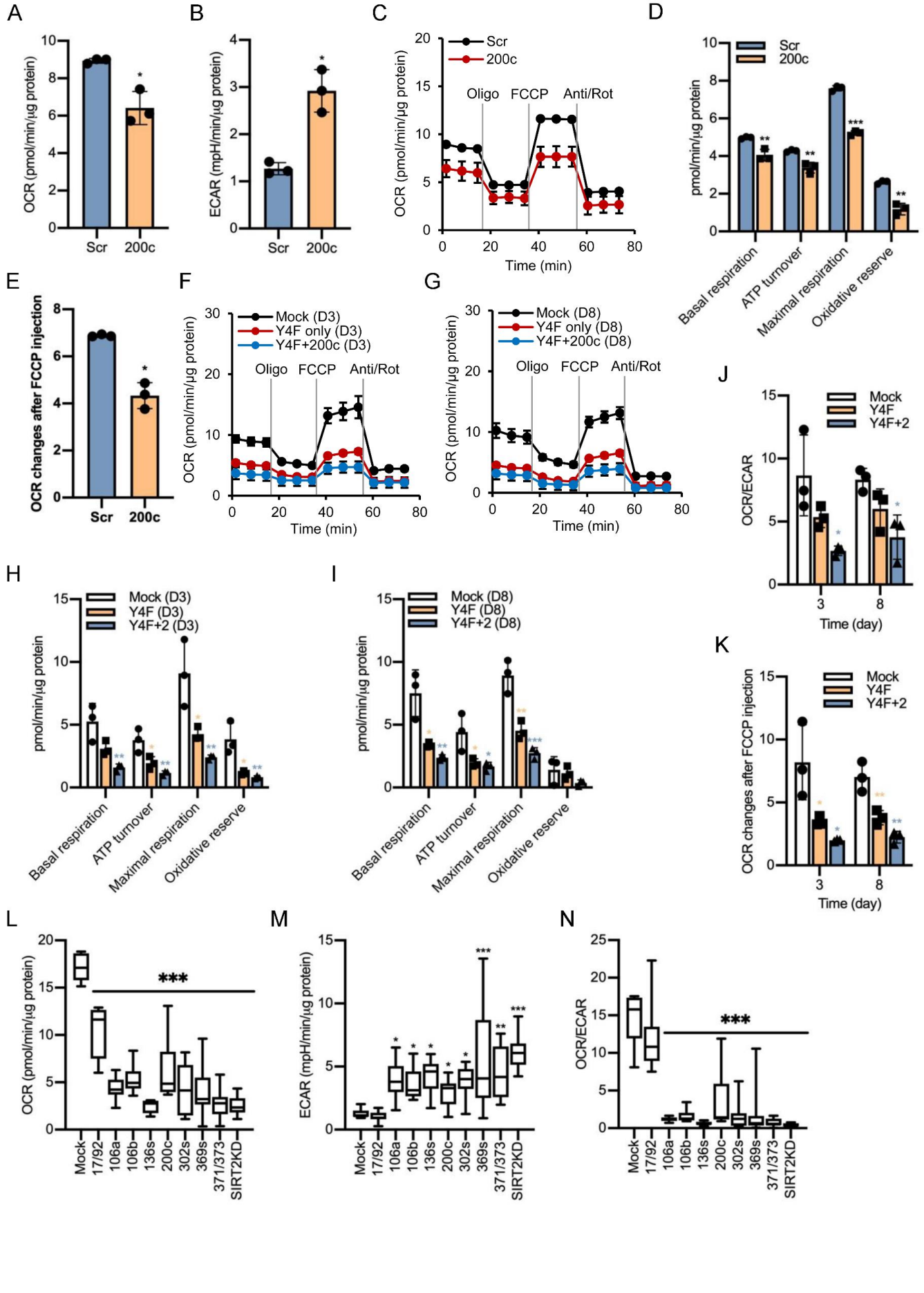
A
OCR (pmol/min/μg protein)
Scr
200c
B
ECAR (mpH/min/μg protein)
C
Scr
200c
Oligo
FCCP
Anti/Rot
Time (min)
D
pmol/min/μg protein
Basal respiration
ATP turnover
Maximal respiration
Oxidative reserve
E
OCR changes after FCCP injection
F
Mock (D3)
Y4F only (D3)
Y4F+200c (D3)
G
Mock (D8)
Y4F only (D8)
Y4F+200c (D8)
H
Mock (D3)
Y4F (D3)
Y4F+2 (D3)
I
Mock (D8)
Y4F (D8)
Y4F+2 (D8)
J
Mock
Y4F
Y4F+2
OCR/ECAR
Time (day)
K
OCR changes after FCCP injection
L
M
N
Mock
17/92
106a
106b
136s
200c
302s
369s
371/373
SIRT2KD

Supplemental Figure 1. Identification of microRNAs regulating metabolic reprogramming and improved reprogramming method based on their combination with Y4F. (A-B) Oxygen consumption rate (OCR) (A) and extracellular acidification rate (ECAR) (B) of hDFs transfected with microRNA mimics for control (Scr) or miR-200c (200c) at 3 days after transfection, were assessed using the XFp analyzer. Mean ± s.d., n = 3, *p<0.05, two-tailed unpaired t-test. (C) OXPHOS capacity of hDFs transfected with Scr or miR-200c 3 days after transfection. Mean ± s.d., n = 3. (D-E) Basal respiration, ATP turnover, maximum respiration, oxidative reserve (D) or relative OCR changes after FCCP injection (E). Mean ± s.d., n = 3, *p<0.05, two-tailed unpaired t-test. (F-G) OCR were shown for hDFs infected with lentiviruses expressing Y4F and/or miR-200c (200c) at 3 (F) or 8 (G) days following transduction. Mean ± s.d., n = 3. (H-I) Basal respiration, ATP turnover, maximum respiration, and oxidative reserve in hDFs at 3 (H) or 8 (I) days following transduction, as shown in F-G. Mean ± s.d., n = 3, * p<0.05; ** p<0.01; *** p<0.005, one-way ANOVA with Tukey's post-test. (J-K) OCR/ECAR ratio (J) or relative OCR changes after FCCP injection (K) in hDFs following transduction, as shown in F-G. Mean ± s.d., n = 3, * p<0.05; ** p<0.01, two-way ANOVA with Tukey's post-test. (L-M) OCR (L) and ECAR (M) in hDFs transduced with lentivirus expressing individual miRNAs at 3 days after transduction. Mean ± s.d., n = 9, * p<0.05; ** p<0.01; *** p<0.005, one-way ANOVA with Tukey's post-test. (N) OCR/ECAR ratio, as shown in L-M. Mean ± s.d., n = 9, *** p<0.005, one-way ANOVA with Tukey's post-test.

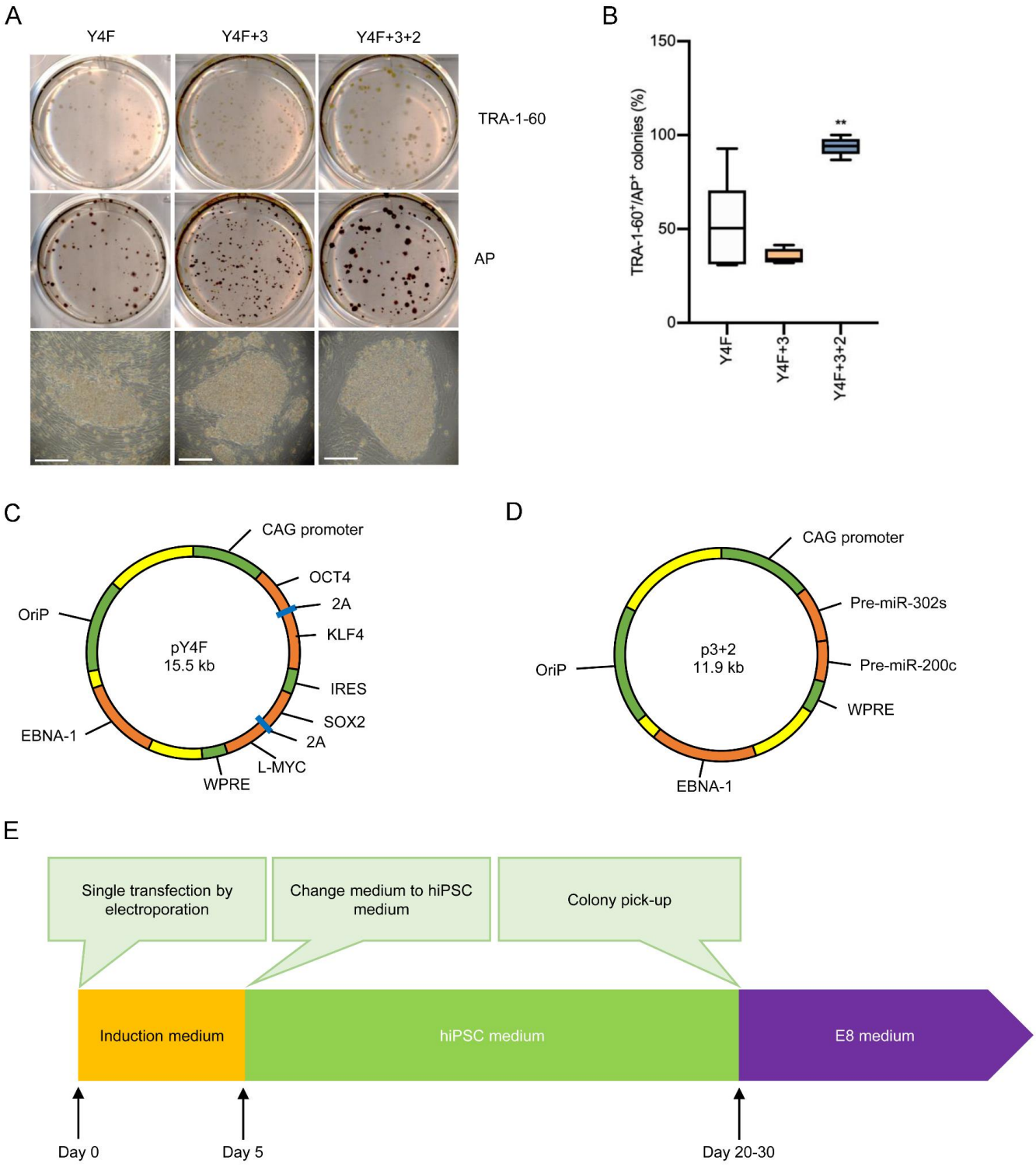

Supplemental Figure 2. Identification of Y4F+3+2 reprogramming protocol. (A) Representative pictures of TRA-1-60 (upper) or AP (lower)-positive colonies at 14 days post-transduction. (B) Percentage of TRA-1-60$^+$ colonies among AP$^+$ colonies following lentiviral transduction of Y4F, Y4F+3, or Y4F+3+2 in human adult fibroblasts (GM03529). Mean ± s.d., n = 6, $^{**}p<0.01$, two-way ANOVA with Tukey's post-test. (C-D) Plasmid maps encoding pY4F (OCT4, SOX2, KLF4, and L-MYC) (C) and miR-302s and -200c (p3+2) (D). (E) Schematic diagram of our established episomal system-based reprogramming method using single transfection with pY4F and pY3+2.

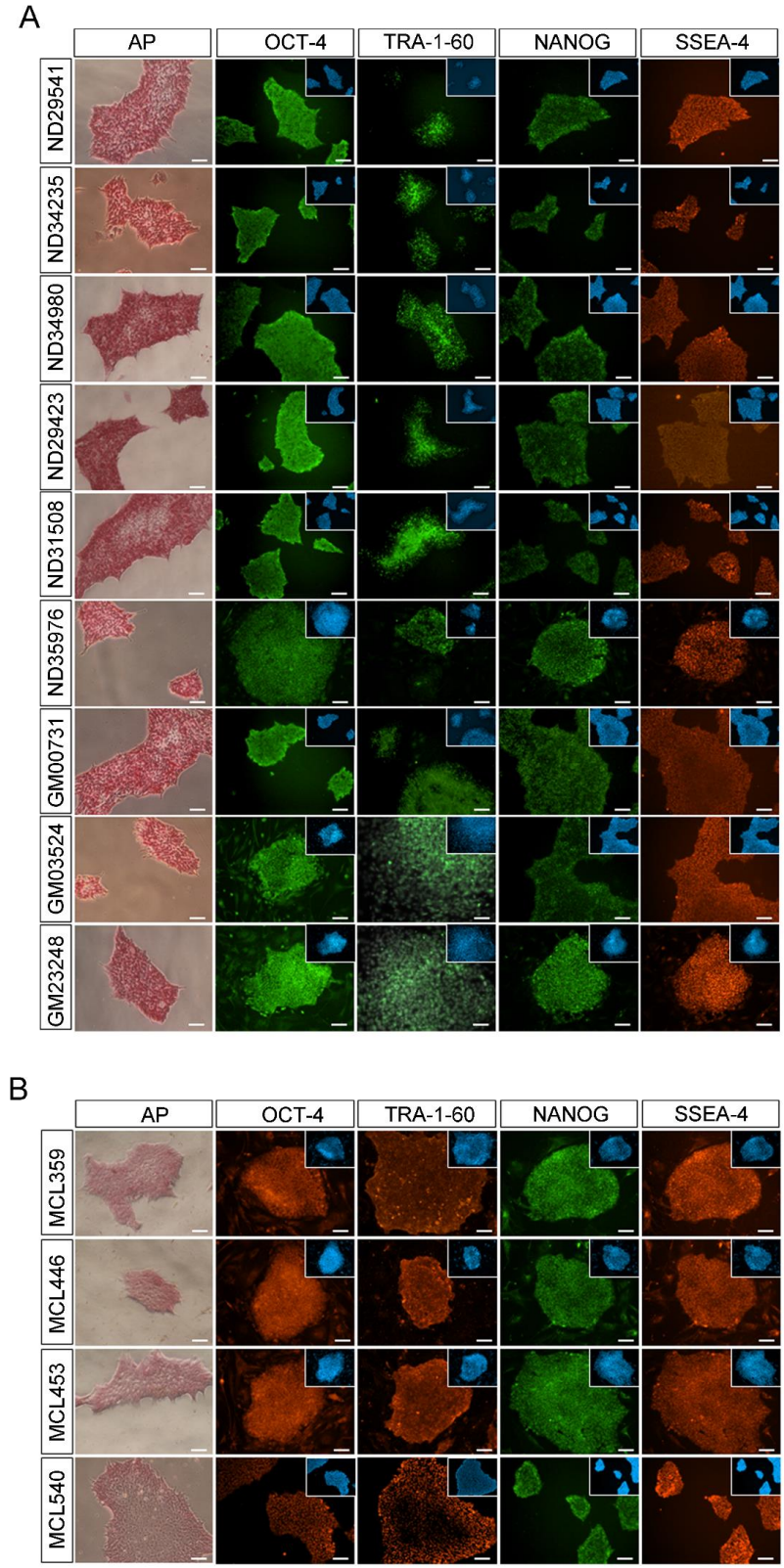

Supplemental Figure 3. Immunocytochemical staining of hiPSC lines generated by our improved reprogramming method. Immunocytochemical staining of human iPSCs generated by our episomal method from various human adult fibroblasts from multiple sources, including 9 fibroblast lines from the Coriell Institute (3 familial PD, 3 sporadic PD, and 3 healthy subjects, A) and 4 samples from new skin biopsies (3 healthy subjects and 1 sporadic PD patient, B).

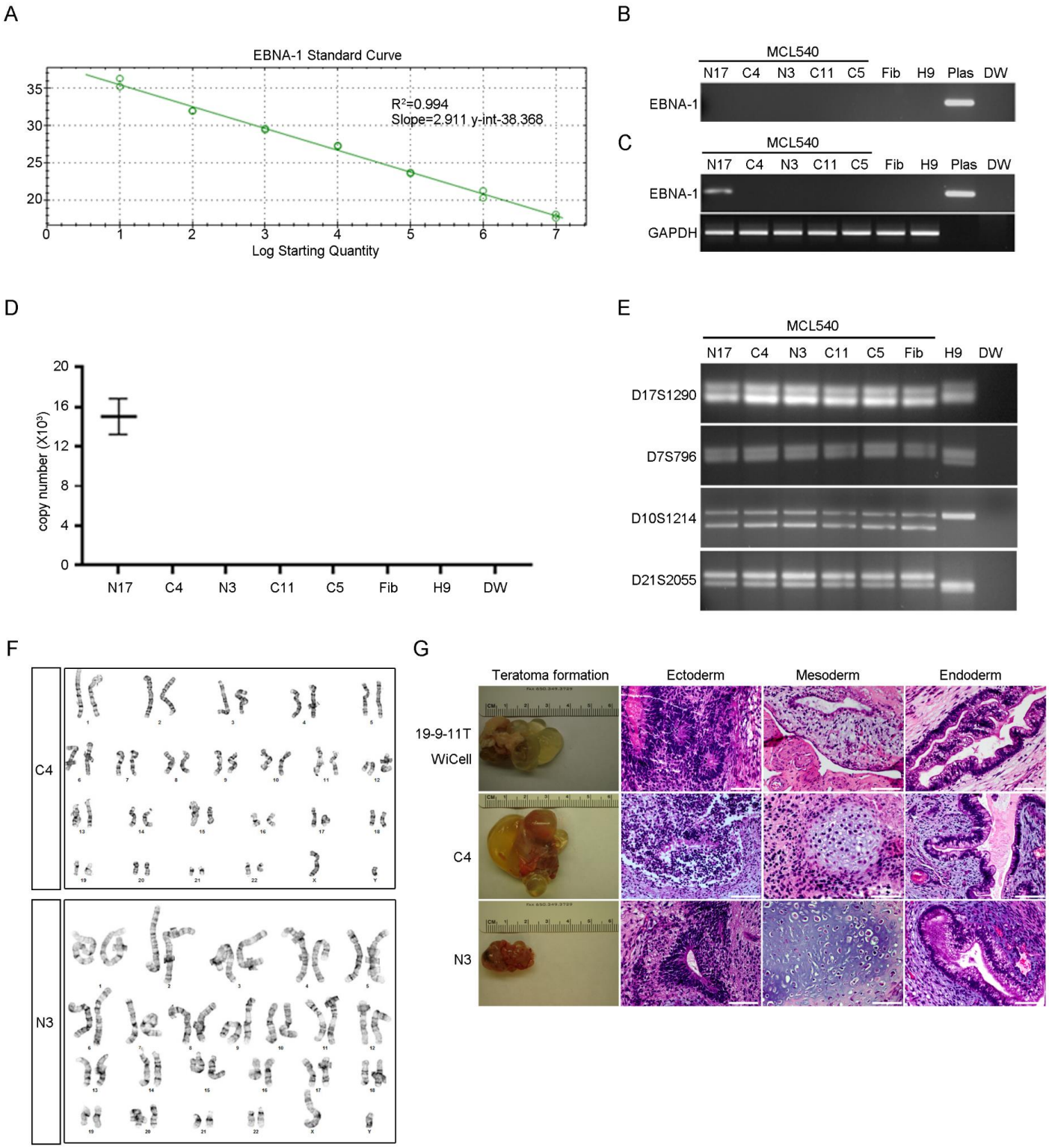
A
EBNA-1 Standard Curve
R²=0.994
Slope=2.911 y-int-38.368
Log Starting Quantity
B
MCL540
N17 C4 N3 C11 C5 Fib H9 Plas DW
EBNA-1
C
MCL540
N17 C4 N3 C11 C5 Fib H9 Plas DW
EBNA-1
GAPDH
D
copy number (X10³)
N17 C4 N3 C11 C5 Fib H9 DW
E
MCL540
N17 C4 N3 C11 C5 Fib H9 DW
D17S1290
D7S796
D10S1214
D21S2055
F
C4
N3
G
Teratoma formation
Ectoderm
Mesoderm
Endoderm
19-9-11T
WiCell
C4
N3

Supplemental Figure 4. Characterization of hiPSC lines generated by our improved reprogramming method. (A) Standard curve of qRT-PCR detection of EBNA-1 specific sequence (EB-01). (B) No residual plasmid DNA was detected in cytoplasm of any hiPSC line. Samples from the original fibroblasts (Fib), a human ESC line (H9), and negative control (distilled water: DW) were also tested. Plasmid-specific primers based on EBNA sequence (EB-01) were used for qRT-PCR analyses. (C) Detection of integrated plasmid DNAs in the host genome. One line (N17) was found to have integrated plasmid DNA sequences in the host chromosomal DNAs. (D) qRT-PCR analysis of integrated plasmid sequences. Mean ± s.d., $n = 3$, ***$p<0.005$, one-way ANOVA. (E) Chromosomal genotyping of hiPSC lines derived from the skin biopsy of a sporadic PD patient (MCL540). Patterns were compared with samples from the original fibroblasts (Fib) and the hESC line (H9) as positive and negative controls, respectively. DW, distilled water. (F) Representative images of C4 and N3 normal karyotype. (G) Representative images of teratoma formation and the three germ layer tissues from the 19-9-11T hiPSC line from WiCell (upper), C4 (middle) and N3 (lower). Scale bar: 100 μm.

A

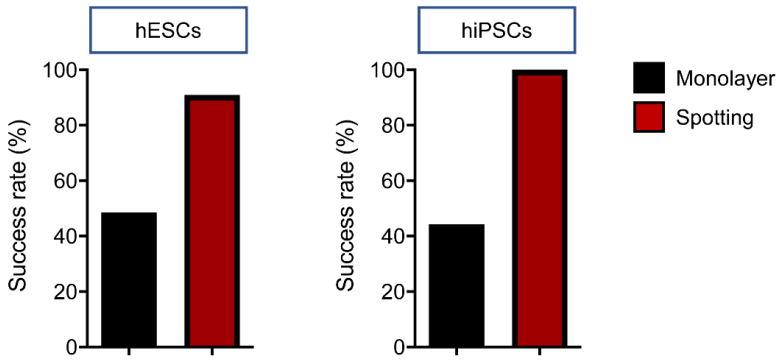

B

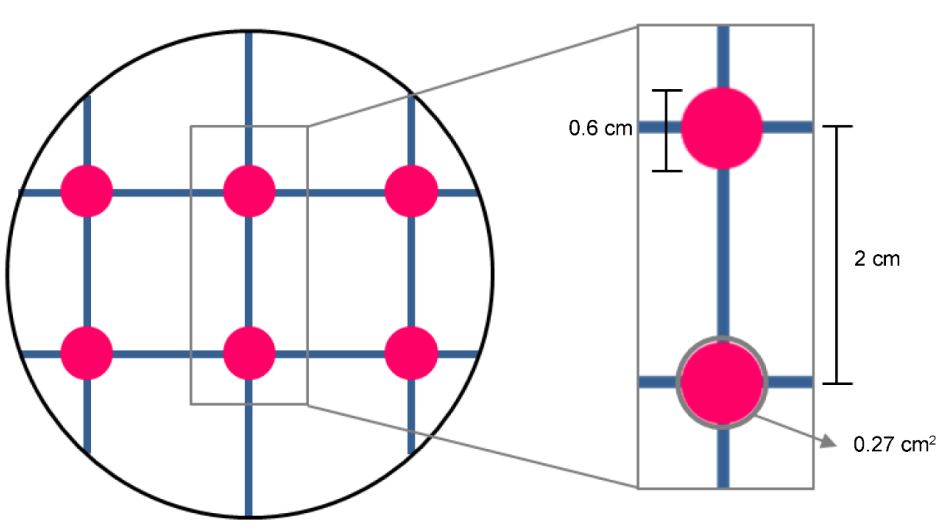

6 cm dish

C

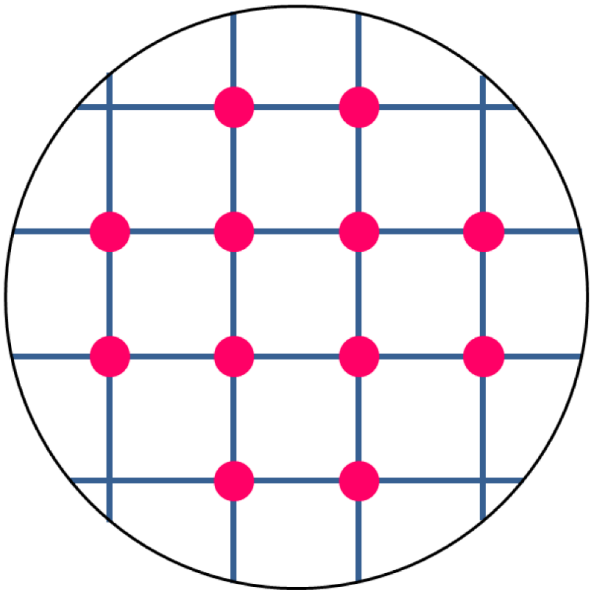

10 cm dish

Supplemental Figure 5. Schematic diagram of spotting-based differentiation protocol. (A) The differentiation success rate of hESCs and hiPSCs using monolayer-based or spotting-based methods (*n* = 76 for hESCs and *n* = 48 for hiPSCs). In vitro differentiation was considered to be a success when 1) cells could survive with >50% confluence at D15 and 2) cells could be harvested and plated on the cover glass for further characterization by ICC. (B-C) Schematic diagram of spotting for the 6-cm culture plate with 6 spots and for the 10-cm culture plate with 12 spots.

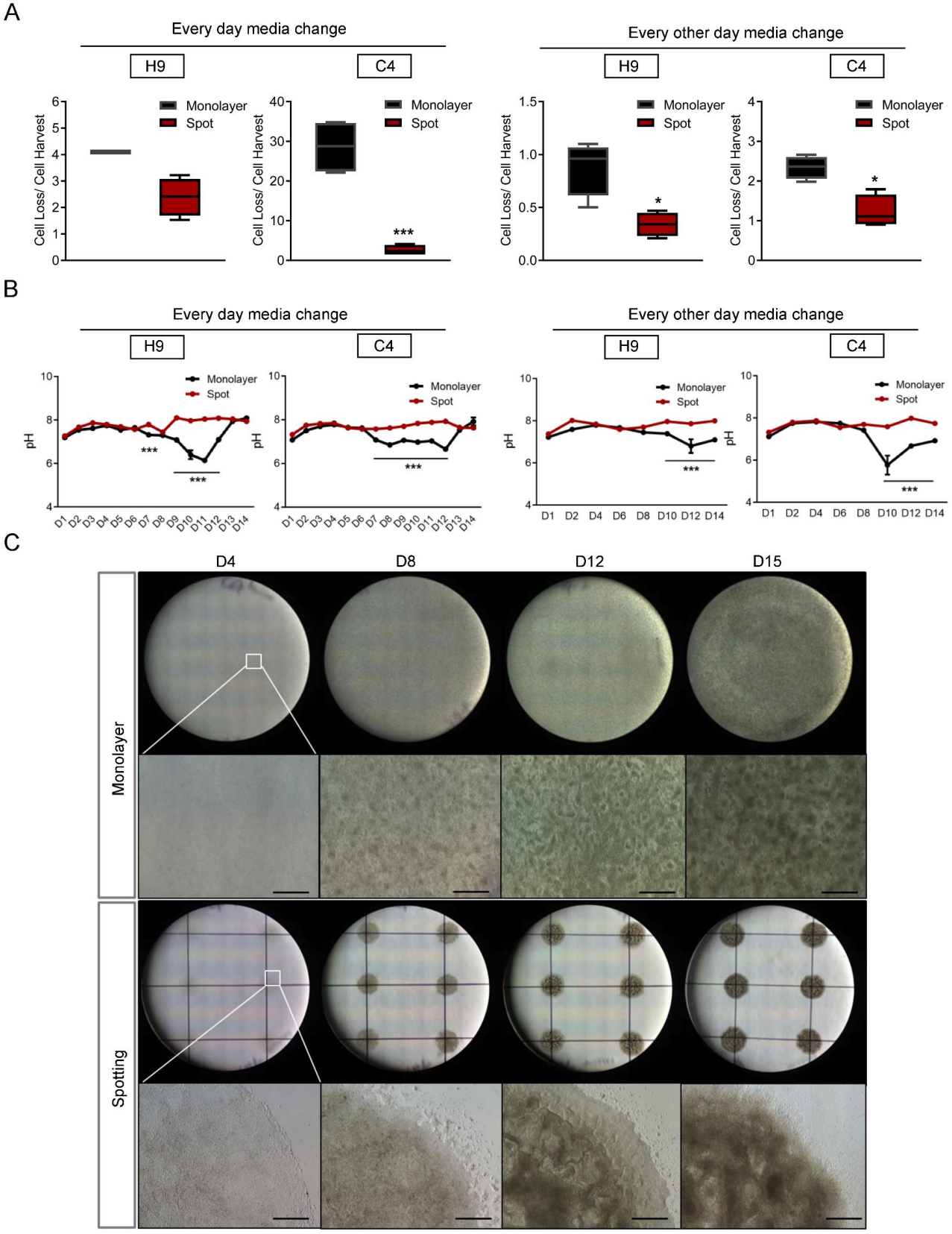
A
Every day media change
H9
C4
Monolayer
Spot
Cell Loss/ Cell Harvest
***
Every other day media change
*
B
pH
D1 D2 D3 D4 D5 D6 D7 D8 D9 D10 D11 D12 D13 D14
D1 D2 D4 D6 D8 D10 D12 D14
C
D4
D8
D12
D15
Monolayer
Spotting

Supplemental Figure 6. Comparison of spotting-based and monolayer-based in vitro differentiation. Using in vitro differentiation in monolayer- and spotting-based methods, comparison of (A) the ratio of cell loss and cell harvest at differentiation D15 on both C4 and H9 (n = 4). The cell numbers of loss and harvest were obtained by FACS; (B) the pH value of supernatant harvested at different time points on both C4 and H9 (n = 4); (C) morphological features at D4, D8, D12 and D15 on C4. The scale bars present 20 μm. Data are presented as mean ± SEM, * p<0.05; *** p<0.005. Two-tailed paired t test (A), one way ANOVA with Tukey's multiple comparisons test (B) were used to determine statistical significance.

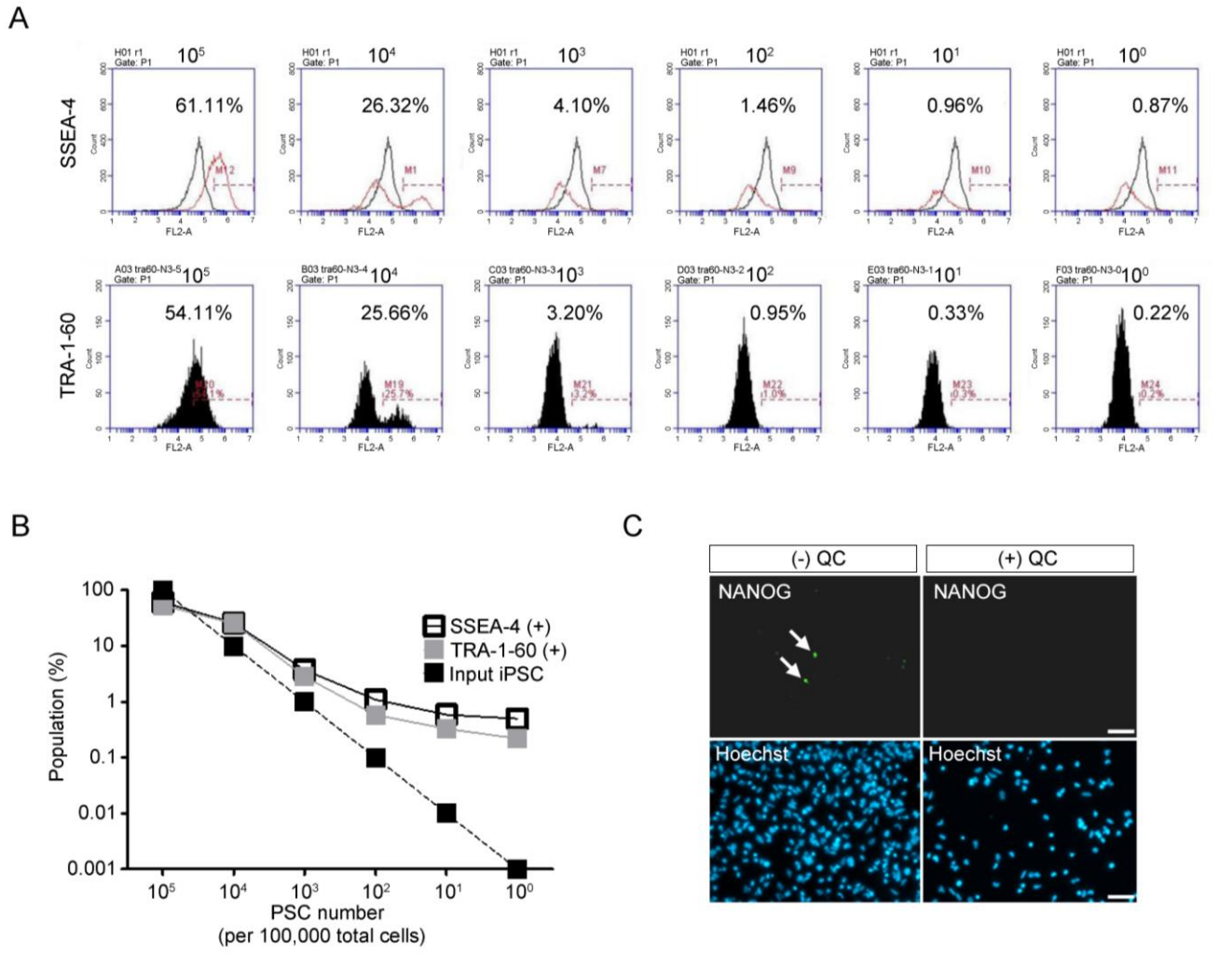

Supplemental Figure 7. Removal of undifferentiated hiPSC by quercetin treatment. (A) Anti-SSEA-4 and TRA-1-60 FACS analyses of undifferentiated hiPSCs serially diluted with fibroblasts by factors of 10 among 100K total cells. (B) Plot of input hiPSC number vs resulting percentage of SSEA-4^{+} and TRA-1-60^{+} cells. (C) Immunostaining for NANOG in D14 cells with or without quercetin treatment. Scale bar: 100 μm.

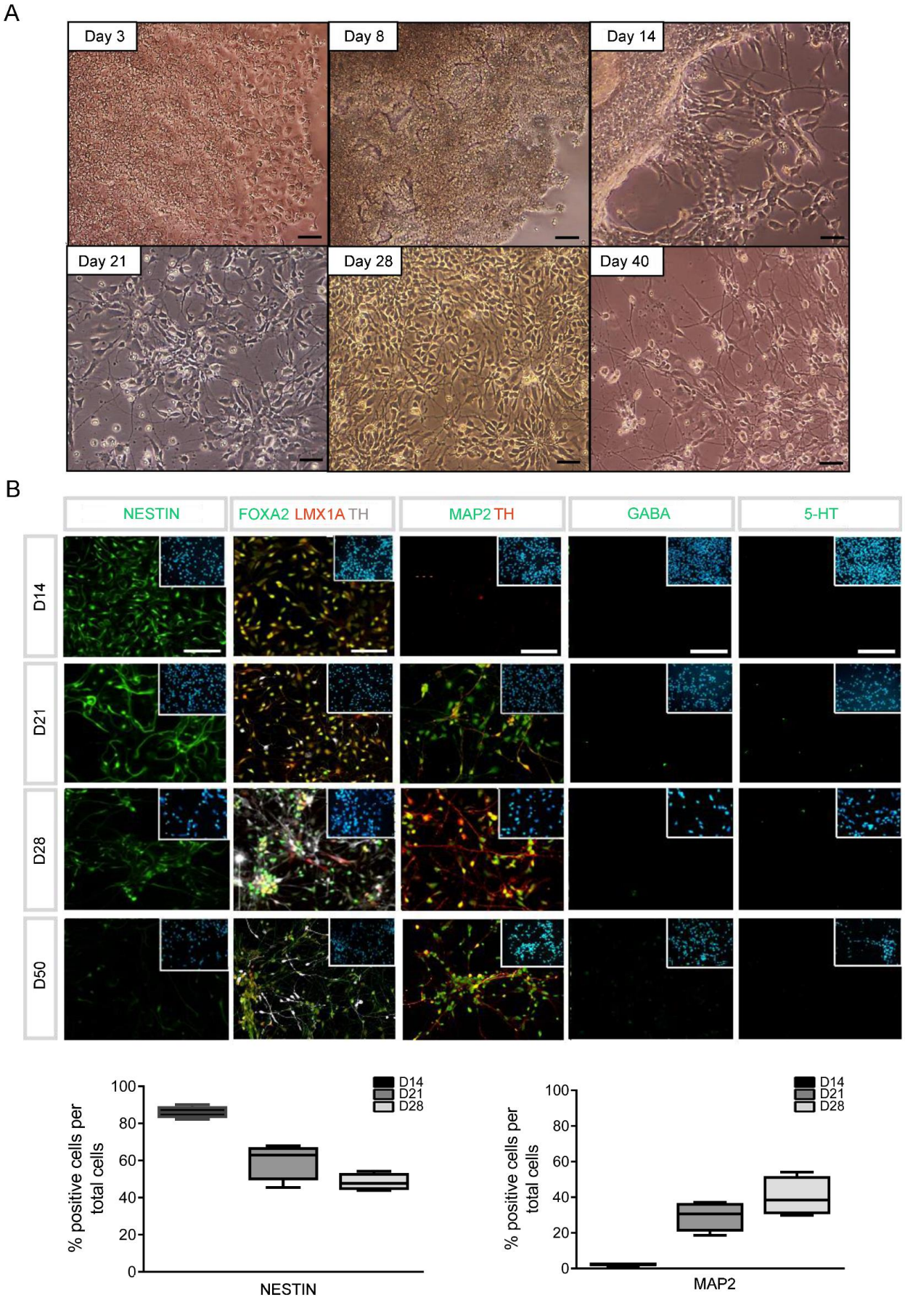
A
Day 3
Day 8
Day 14
Day 21
Day 28
Day 40
B
NESTIN
FOXA2 LMX1A TH
MAP2 TH
GABA
5-HT
D14
D21
D28
D50
% positive cells per total cells
100
80
60
40
20
0
D14
D21
D28
NESTIN
% positive cells per total cells
100
80
60
40
20
0
D14
D21
D28
MAP2

Supplemental Figure 8. Characterization of *in vitro* differentiated C4 hiPSC. (A) Bright-field images of differentiated cells from D3 to D40. (B) Immunofluorescence staining and percentage of neural precursor (NESTIN), mDAP (FOXA2/LMX1A), mDAN (MAP2 and TH), GABAergic neurons (GABA) and serotonergic neurons (5-HT) positive cells and during mDA differentiation D14, D21, D28 and D50. Scale bar: 100 µm. Data are presented as mean ± SEM, *n* = 6.

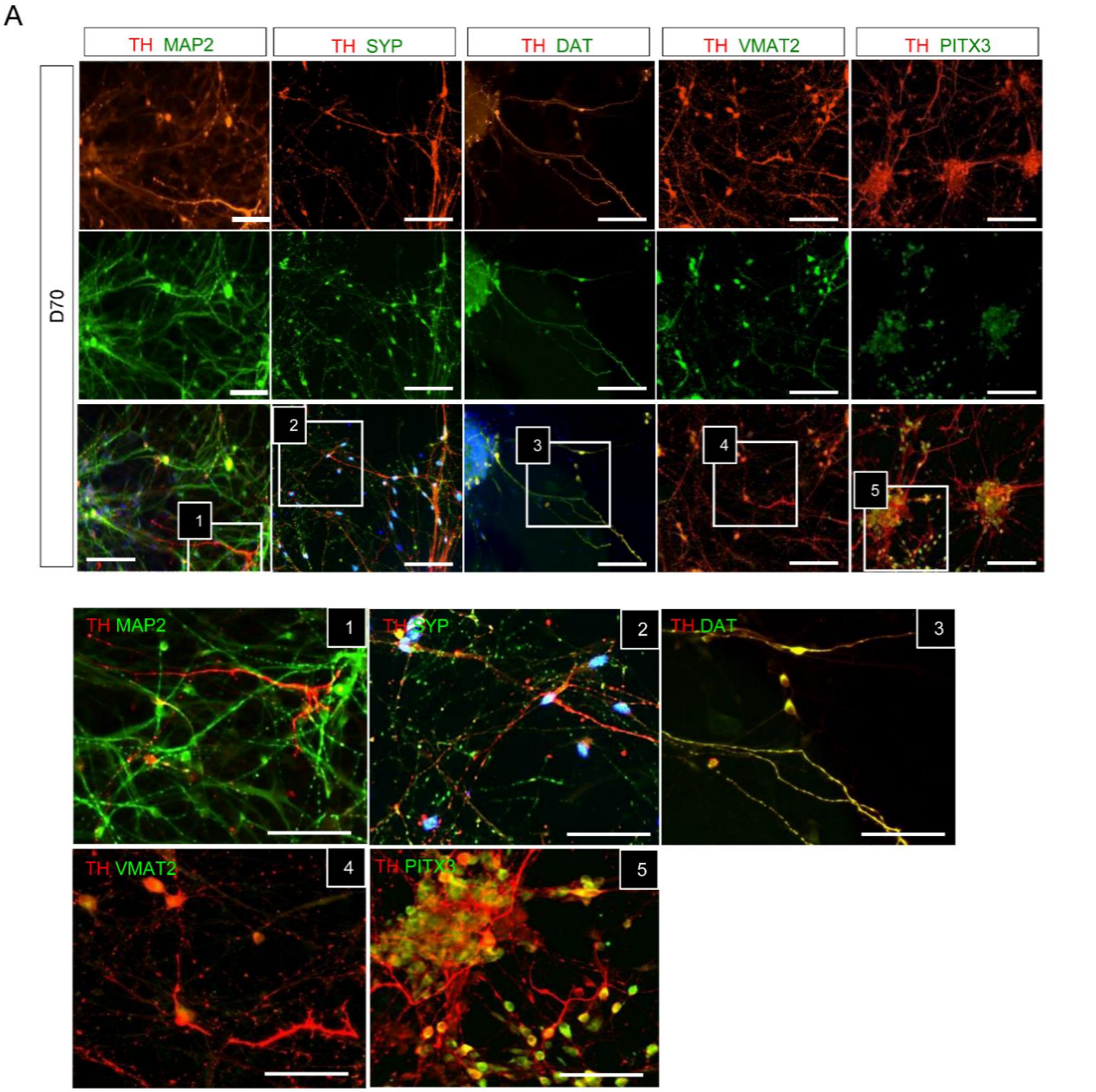
A
TH MAP2
TH SYP
TH DAT
TH VMAT2
TH PITX3
D70
1
2
3
4
5
TH MAP2
TH SYP
TH DAT
TH VMAT2
TH PITX3
B
ALDH1A1 GIRK2
TH
ALDH1A1
GIRK2
TH ALDH1A1 GIRK2
ALDH1A1 CALB
TH
ALDH1A1
CALBINDIN
TH ALDH1A1 CALBINDIN

Supplemental Figure 9. Cell fate analysis of in vitro differentiated C4 hiPSC. (A) Immunofluorescence staining of D70 cells recorded electrophysiologically, co-expressing TH, MAP2, SYP (Synaptophysin), DAT (Dopamine transporter), VMAT2 (Vesicular monoamine transporter 2) and PITX3. Scale bar: 100 µm. (B) Immunofluorescence staining of ALDH1A1, GIRK2 and Calbindin with TH positive cells. Scale bar: 100 µm.

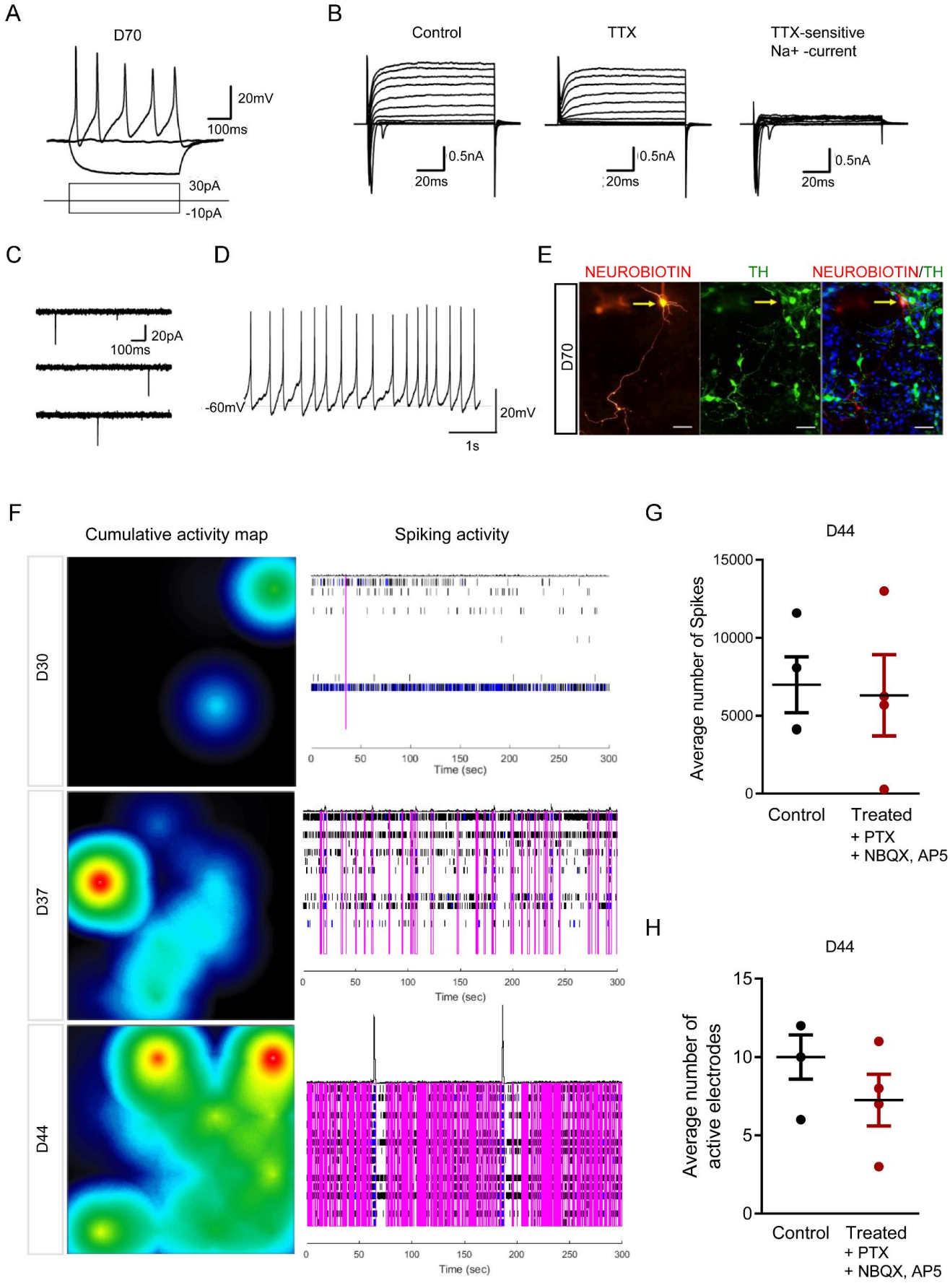
A
D70
20mV
100ms
30pA
-10pA
B
Control
TTX
TTX-sensitive
Na+ -current
0.5nA
20ms
C
20pA
100ms
D
-60mV
20mV
1s
E
NEUROBIOTIN
TH
NEUROBIOTIN/TH
D70
F
Cumulative activity map
Spiking activity
D30
D37
D44
0
50
100
150
200
250
300
Time (sec)
G
D44
Average number of Spikes
15000
10000
5000
0
Control
Treated
+ PTX
+ NBQX, AP5
H
D44
Average number of active electrodes
15
10
5
0
Control
Treated
+ PTX
+ NBQX, AP5

Supplemental Figure 10. Electrophysiological features of *in vitro* differentiated C4 hiPSC. (A) Representative voltage traces of action potentials induced by depolarizing current injection (500 ms) on D70. (B) Representative current traces evoked by voltage pulses in voltage-clamp mode. Left: transient inward and sustained outward currents induced by voltage pulses from -70 mV to +40 mV in 10 mV increments (100 ms duration). Middle: inward currents were completely blocked by TTX (1 µM). Right: traces recorded in the presence of TTX were subtracted from the traces recorded under control conditions to isolate voltage-gated Na^+ currents at different membrane potentials. (C) Spontaneous postsynaptic currents recorded at -70 mV in voltage-clamp mode. (D) Spontaneous firing of differentiated cells in current-clamp mode at the resting membrane potential. (E) Immunofluorescence staining of individual recorded cells. Neurobiotin-filled cell (red) shows TH positivity (green). Scale bar: 100 µm. (F) Cumulative activity map and spiking activity of in vitro differentiated C4 hiPSC at D30, D37 and D44 using the multi-electrode array. (G-H) The average spikes number (G) and the active electrodes numbers (H) of D44 differentiated C4 hiPSC with or without treatment with a combination of glutamate receptor antagonists, NBQX + AP5, and a GABAA receptor antagonist, Picrotoxin. Data are presented as mean ± SEM, $n = 4$.

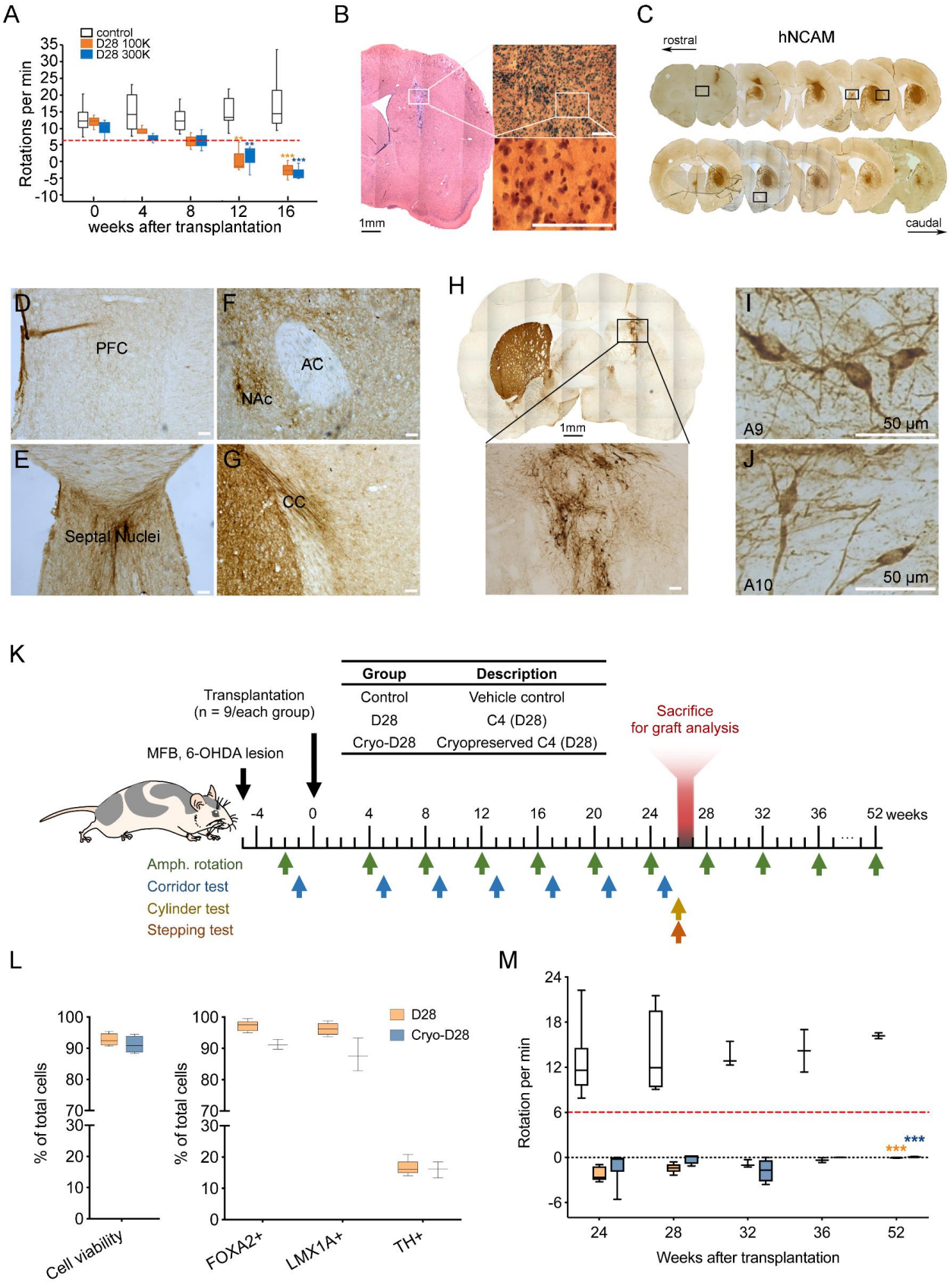
A
control
D28 100K
D28 300K
Rotations per min
weeks after transplantation
B
1mm
C
rostral
hNCAM
caudal
D
PFC
F
AC
NAc
E
Septal Nuclei
G
CC
H
1mm
I
A9
50 µm
J
A10
50 µm
K
Group
Description
Control
Vehicle control
D28
C4 (D28)
Cryo-D28
Cryopreserved C4 (D28)
Transplantation
(n = 9/each group)
MFB, 6-OHDA lesion
Sacrifice
for graft analysis
-4
0
4
8
12
16
20
24
28
32
36
52 weeks
Amph. rotation
Corridor test
Cylinder test
Stepping test
L
% of total cells
Cell viability
D28
Cryo-D28
FOXA2+
LMX1A+
TH+
M
Rotation per min
Weeks after transplantation

Supplemental Figure 11. Analyses of in vivo transplantation outcomes in athymic rat models of PD. (A) 6-OHDA lesioned Taconic rats Amphetamine induced rotation test before and after transplantation with C4-derived D28 DA progenitors (100,000 or 300,000 cells) at 4, 8, 12 and 16 weeks. Data are presented as mean ± SEM. ** means p< 0.01, *** means p<0.001. (B) H&E staining of athymic rat brains 6 months following transplantation with Day 28 cells. (C) Immunohistochemistry of hNCAM reveals extensive fiber outgrowth into multiple areas throughout the host brain in successive coronal sections. (D-G) Higher magnification of hNCAM staining illustrates outgrowth patterns from the graft into prefrontal cortex (D), septal nuclei (E), nucleus accumbens (F), and corpus callosum(G). (H-J) Histological analysis at 6 months post transplantation, of TH^+ dopaminergic neurons in the grafts produced by D28 DA progenitors. Note A9-like neuronal morphology with large, angular cell somata (I) as well as smaller spherical A10-like neurons (J). (K) Schematic diagram of in vivo Charles River athymic rat experiments. (L) Comparison of cell viability and FOXA2, LMX1A and TH positive cell numbers between freshly prepared D28 cells and Cryo-D28 cells thawed after 1 week in liquid nitrogen (n = 3-4). (M) Amphetamine-induced rotation test from 24 to 52 weeks after D28 cells and Cryo-D28 cells transplantation (n = 3-4). Data are presented as mean ± SEM. *p < 0.05, **p < 0.01, ***p < 0.001, Student's t-test. AC, anterior commissure; cc, corpus callosum; NAc, nucleus accumbens; PFC, prefrontal cortex. All scale bars indicate 100 μm unless specified description.

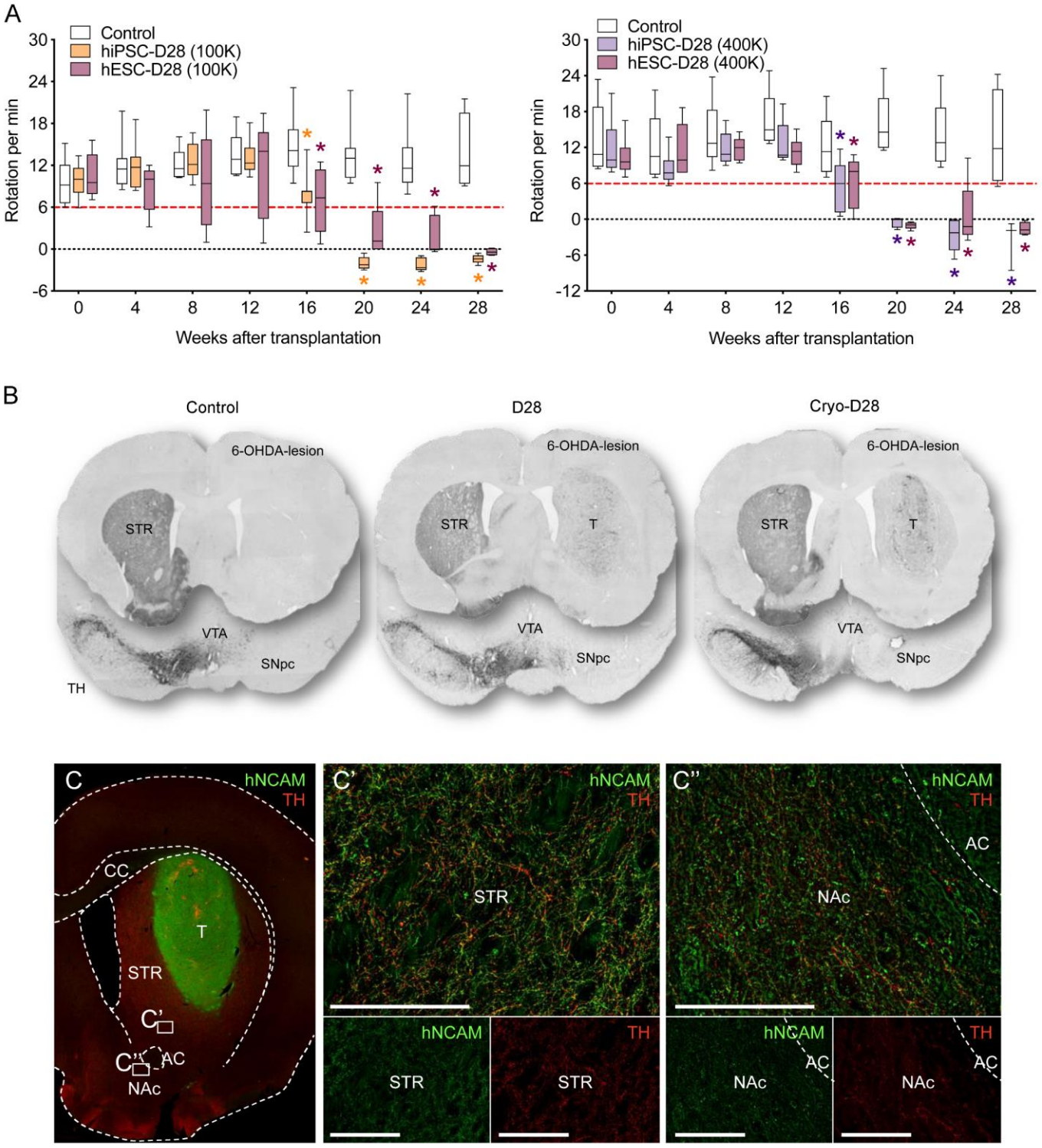

Supplemental Figure 12. Function and innervation analyses of in vivo transplantation. (A) Amphetamine-induced rotation test following transplantation of H9 hESC- and C4 hiPSC-derived D28 cells (*n* = 5-8). (B) Representative images of 6-OHDA lesioned brains from each group. (C) High magnification image of graft innervation into STR and NAc. Data are presented as mean ± SEM. **p* < 0.05, ***p* < 0.01, ****p* < 0.001, Student's *t*-test. STR, striatum; NAc, nucleus accumbens.

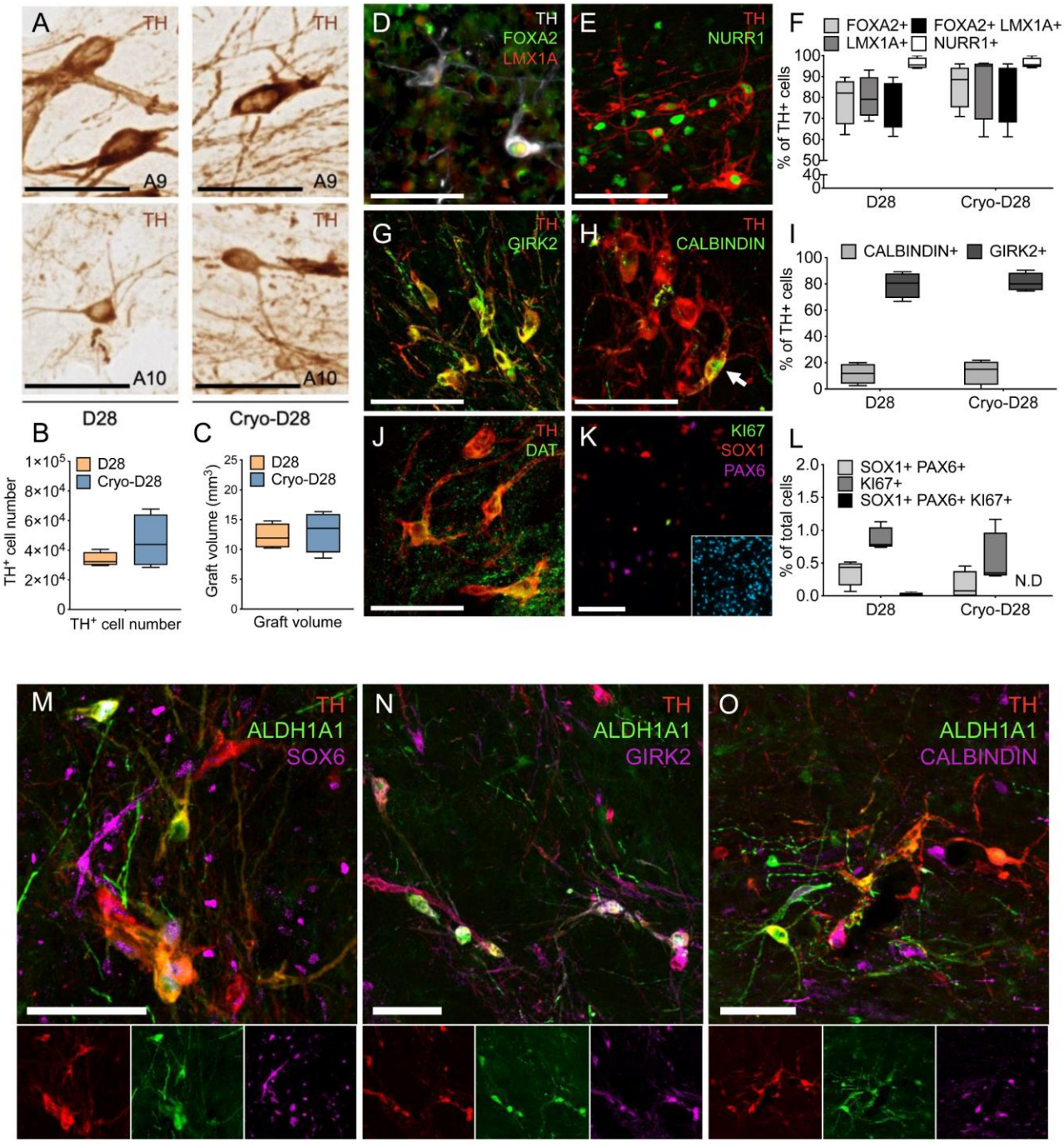
A
TH
A9
A10
D28
Cryo-D28
B
C
D28
Cryo-D28
TH+ cell number
Graft volume (mm3)
Graft volume
D
TH
FOXA2
LMX1A
E
TH
NURR1
F
FOXA2+
FOXA2+ LMX1A+
LMX1A+
NURR1+
% of TH+ cells
G
TH
GIRK2
H
TH
CALBINDIN
I
CALBINDIN+
GIRK2+
J
TH
DAT
K
KI67
SOX1
PAX6
L
SOX1+ PAX6+
KI67+
SOX1+ PAX6+ KI67+
% of total cells
N.D
M
TH
ALDH1A1
SOX6
N
TH
ALDH1A1
GIRK2
O
TH
ALDH1A1
CALBINDIN

Supplemental Figure 13. Graft analyses after transplantation of C4-derived mDA cells. (A) Immunostaining of TH^+ neurons (both A9- and A10-like) in D28 and Cryo-D28 grafts. (B) Estimation of number of surviving TH^+ neurons in D28 and Cryo-D28 grafts (*n* = 4). (C) Estimation of graft volume in D28 and Cryo-D28 grafts (*n* = 4). (D-F) Immunofluorescence co-staining for FOXA2, LMX1A (D) and NURR1 (E) and TH in D28 grafts (*n* = 4). (F) Quantification of TH^+ neurons that co-express FOXA2, LMX1A, both makers, or NURR1 in D28 and Cryo-D28 grafts (*n* = 4). (G) Immunofluorescence co-staining for DAT and TH. (H) Immunofluorescence staining for PAX6, SOX1 and Ki67 in grafted neurons. (I) Quantification of $PAX6^+$, $SOX1^+$ and $Ki67^+$ cells in D28 and Cryo-D28 grafts (*n* = 4). (J-L) Immunofluorescence co-staining of $GIRK2^+$ (J) and $calbindin^+$ (K) neurons for TH in D28 and Cryo-D28 grafts (*n* = 4). (L) Quantification of $calbindin^+$ and $GIRK2^+$ neurons in D28 and Cryo-D28 grafts. (M-O) Immunofluorescence co-staining of TH^+, $ALDH1A1^+$ and $SOX6^+$ (M), TH^+, $ALDH1A1^+$ and $GIRK2^+$ (N), TH^+, $ALDH1A1^+$ and $CALBINDIN^+$ (O) in D28 grafts. All graft analysis data of Taconic rats (B-J) were obtained 18 weeks after transplantation. All graft analysis data of Charles River rats (O-S) were obtained 26 weeks after transplantation. AC, anterior commissure; cc, corpus callosum; NAc, nucleus accumbens; PFC, prefrontal cortex; SNpc, substantia nigra pars compacta; STR, striatum; T, transplant; VTA, ventral tegmental area. Scale bars: 50 µm (A);100 µm (D-O).

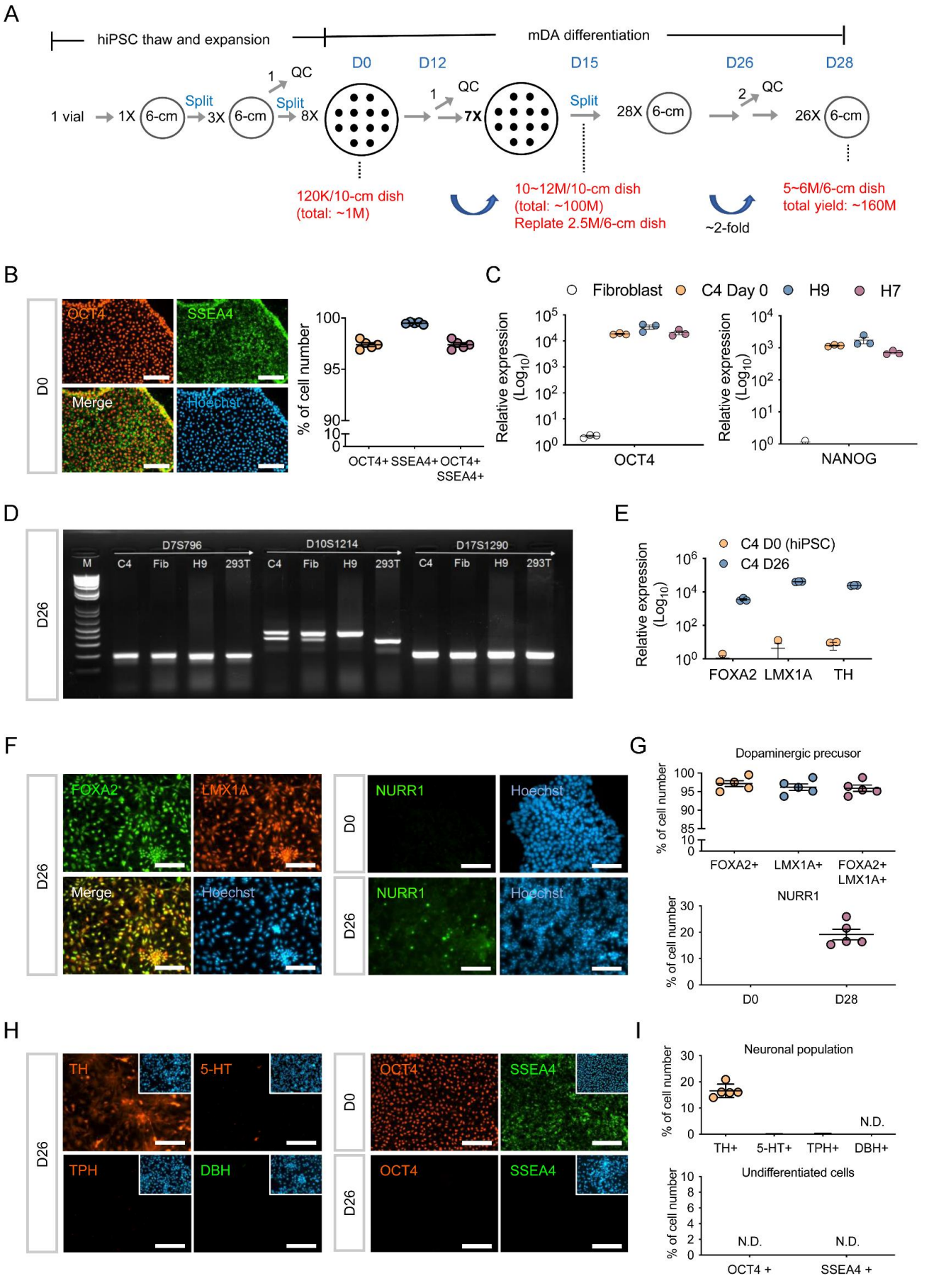
A
hiPSC thaw and expansion
mDA differentiation
D0
D12
D15
D26
D28
1 vial
1X
6-cm
Split
3X
6-cm
Split
8X
1
QC
1
QC
7X
Split
28X
6-cm
2
QC
26X
6-cm
120K/10-cm dish
(total: ~1M)
10~12M/10-cm dish
(total: ~100M)
Replate 2.5M/6-cm dish
~2-fold
5~6M/6-cm dish
total yield: ~160M
B
D0
OCT4
SSEA4
Merge
Hoechst
% of cell number
OCT4+
SSEA4+
OCT4+ SSEA4+
C
Fibroblast
C4 Day 0
H9
H7
Relative expression (Log10)
OCT4
NANOG
D
D26
M
C4
Fib
H9
293T
D7S796
D10S1214
D17S1290
E
C4 D0 (hiPSC)
C4 D26
Relative expression (Log10)
FOXA2
LMX1A
TH
F
D26
FOXA2
LMX1A
Merge
Hoechst
D0
D26
NURR1
Hoechst
G
Dopaminergic precusor
% of cell number
FOXA2+
LMX1A+
FOXA2+ LMX1A+
NURR1
D0
D28
H
D26
TH
5-HT
TPH
DBH
D0
D26
OCT4
SSEA4
I
Neuronal population
% of cell number
N.D.
TH+
5-HT+
TPH+
DBH+
Undifferentiated cells
N.D.
N.D.
OCT4 +
SSEA4 +

Supplemental Figure 14. GMP differentiation protocol schematic overview and quality control results. (A) Schematic overview of GMP differentiation protocol with cell yield at each stage shown in red. QC indicates quality control. (B) D0 immunocytochemistry QC staining for OCT4 and SSEA-4. (C) D0 QC for Oct4 and Nanog mRNA expression levels using qRT-PCR. (D) C4 D26 DNA fingerprinting QC showing the same patterns as the original fibroblasts, while the negative controls are different, confirming that the C4 iPS cells from the working cell bank originate from the patient's fibroblasts. Fib: fibroblast. M: DNA markers. (E) D26 QC for FOXA2, LMX1A and TH mRNA expression level using qRT-PCR. (F) D26 immunocytochemistry QC staining for FOXA2, LMX1A and Nurr1 using D0 undifferentiated cells as negative control. (G) Quantification of FOXA2, LMX1A and Nurr1 expression from (F). (H) D26 immunocytochemistry quality control staining for TH, 5-HT, TPH, OCT4 and SSEA-4 staining Do undifferentiated cells for OCT4 and SSEA-4 as negative control. (I) Quantification of TH, 5-HT, TPH, OCT4 and SSEA-4 expression from (H). Some cells were harvested at D26 for immunocytochemistry QC to allow cells to adhere to cover slips and complete the staining and analysis process before the final harvest at D28. Scale bar: 100 μm. n = 3 for each experiment.

Supplemental Table 1. Comparison of hiPSC lines derived from newborn (BJ) or adult fibroblasts (GM03529) by different combinations of factors on lentiviral or episomal vectors

Combination of factors	The ratio of TRA-1-60$^+$/AP$^+$			Metabolic change evidence	Pluripotency marker gene expression	Differentiation potential
	Lentiviral vector		Episomal vector			
	BJ	GM03529	BJ	BJ	BJ	BJ
Y4F	42.4±17.4%	53.2±23.2%	49.9±10.8%	~8 days post-infection	Similar to H9 hESC	Skewed differentiation
Y4F+3	44.2±8.8%	35.4±3.8%	50.4±15.6%	~8 days post-infection	Similar to H9 hESC	Skewed differentiation
Y4F+3+2	94.8±1.8%	93.9±4.7%	91.7±9.8%	~4 days post-infection	Similar to H9 hESC	Unskewed differentiation

Supplemental Table 2. Summary of episomal plasmid-based hiPSC generation

source	subtype	cell ID	age (years)	gender	race	starting Cell No.	# iPS-like colony	efficiency (/initial)	initial P/U	# final iPS lines
Coriell	Familial PD	ND29541	65	Male	Caucasian	5.0E+04	130	0.260%	12	5
Coriell	Familial PD	ND34235	71	Male	Caucasian	5.0E+04	67	0.134%	6	3
Coriell	Familial PD	ND34980	58	Male	Caucasian	5.0E+04	131	0.262%	12	4
Coriell	Sporadic PD	ND29423	73	Male	Caucasian	5.0E+04	187	0.374%	24	6
Coriell	Sporadic PD	ND31508	71	Male	Caucasian	5.0E+04	92	0.184%	12	4
Coriell	Sporadic PD	ND35976	63	Male	Caucasian	5.0E+04	118	0.236%	24	10
Coriell	Healthy	GM00731	96	Male	Caucasian	5.0E+04	181	0.362%	24	5
Coriell	Healthy	GM03524	67	Female	Black	5.0E+04	153	0.306%	24	7
Coriell	Healthy	GM23248	55	Male	Caucasian	5.0E+04	84	0.168%	12	7
Biopsy	Healthy	MCL359	25	Male	N/A	2.0E+04	32	0.160%	12	4
Biopsy	Healthy	MCL446	20	Male	N/A	2.0E+04	37	0.185%	12	5
Biopsy	Healthy	MCL453	22	Female	N/A	2.0E+04	20	0.100%	6	3
Biopsy	Sporadic PD	MCL540	68	Male	Hispanic	2.0E+04	62	0.340%	36	11

Supplemental Table 3. Summary of MCL540-derived hiPSC lines

iPSC lines	Pluripotency markers expression	Chromosome integration	In vitro 3-germ differentiation	Karyotype	Teratoma formation	Whole exome sequencing
N17	Passed	Failed	N/A	N/A	N/A	N/A
C4	Passed	Passed	Passed	46, XY	Passed	Enrolled
N3	Passed	Passed	Passed	46, XY	Passed	Enrolled
C11	Passed	Passed	Passed	46, XY	N/A	Enrolled
C5	Passed	Passed	Passed	46, XY	N/A	Enrolled

Supplemental Table 4. **Numbers of somatic mutations discovered in iPSC lines**

On average, 126 somatic mutations were identified in each of the four iPSC lines (range 92-205). C4 and N3 had fewer somatic mutations compared to the other iPSC lines. ‘Singleton mutations’ shows mutations specific to each iPSC line. Somatic mutations found in the COSMIC database represent mutations reported in various cancer cells, and mutations supported by multiple lines of evidence from COSMIC are shown in parentheses. Mutations in coding regions of the Cancer Gene Census (CGC) genes represent mutations considered to be causal for cancer. However, no somatic mutations identified in the iPSC lines matched tumorigenic mutations among the CGC genes. Lastly, some mutations appear to be present in a fraction of cells with biased allelic ratios (marked as ‘Y’ in ‘Sub-clonal’ column). Please see the Excel Sheet.

Supplemental Table 5. Cell loss and yield by monolayer and spotting-based methods. Comparison between monolayer-based methods with 3 different cell densities (34,000/cm^2, 11,000/cm^2, 3,500/cm^2) and spotting-based methods with 3 different cell densities (40,000/spot, 10,000/spot, 2,500/spot) for level of cell loss during in vitro differentiation of H9 and C4. Detached cells present in the supernatants following medium changes were counted using FACS.

		Density	D0	D1	D2	D4	D6	D8	D10	D12	D14	Cell loss	Cell yield
H9	monolayer	34K/cm^2	730K	70K±11	39K±5	154K±35	816K±170	511K±57	313K±71	1,071K±348	2,373K±376	5,358K±340	1,726K±104
		11K/cm^2	240K	17K±3	28K±8	57K±14	351K±46	1,282K±574	720K±104	793K±170	1,923K±394	5,172K±468	3,582K±186
		3.5K/cm^2	60K	11K±1	14K±3	51K±43	873K±209	337K±119	102K±6	115K±32	1,433K±415	2,937K±325	358K±20
	spotting	40K/spot	240K	52K±31	6K±1	186K±48	317K±45	135K±16	231K±22	2,098K±520	2,498K±289	5,522K±452	6,124K±194
		10K/spot	60K	16K±4	11K±5	109K±43	345K±65	151K±15	172K±20	131K±7	936K±63	1,871K±125	6,434K±124
		2.5K/spot	15K	6K±0	2K±0	10K±2	122K±29	11K±14	5K±2	7K±2	5K±2	167K±16	1,600K±182
C4	monolayer	34K/cm^2	730K	73K±8	190K±56	164K±25	994K±177	1,544K±166	351K±57	1,298K±283	1,373K±215	5,988K±584	3,200K±98
		11K/cm^2	240K	26K±1	27K±3	50K±13	1,136K±173	692K±55	124K±23	926K±214	256K±74	3,236K±288	4,251K±99
		3.5K/cm^2	60K	12K±1	9K±1	14K±1	562K±109	833K±59	677K±272	1,173K±118	566K±124	3,845K±432	1,165K±83
	spotting	40K/spot	240K	5K±0	17K±2	71K±14	223K±33	210K±17	85K±14	1,259K±314	1,012K±216	2,882K±345	6,191K±268
		10K/spot	60K	2K±1	7K±1	27K±3	159K±13	167K±21	53K±11	1,498K±289	979K±132	2,891K±257	7,622K±141
		2.5K/spot	15K	2K±1	3K±0	4K±0	45K±11	83K±13	30K±2	60K±3	153K±20	381K±42	3,493K±213

Supplemental Table 6. Survival and Function of hiPSC-derived dopamine cells in rat brain

References	Cell stage	Rat host strain	Grafted cell number	Avg. DA yield (TH^+/100,000) (period)	D-Amp rotation recovery % (period)	Corridor test recovery% (period)	Cylinder test recovery% (period)	Stepping test recovery% (period)
This study	D28	Athymic (CR)	1 $X10^5$	34,560 ± 3,200 (24w)	~ 130% (16-52w)	~ 40% (16-24w)	~ 40% (24w)	~ 60% (24w)
	D28 (cryo)	Athymic (CR)	1 $X10^5$	46,094 ± 8,967 (24w)	~ 130% (16-52w)	~ 30% (16-24w)	~ 30% (24w)	~ 70% (24w)
	D28	Athymic (Taconic)	1 $X10^5$	5,621 ± 1029 (16w)	~ 125% (8-16w)	N/A	N/A	N/A
64	D20	SD	N/A	2,106 ±313/mm^3 (12w)*	~ 40% (12w)	N/A	N/A	N/A
57	D42	SD	4 $X10^5$	1,222 ± 160 (16w)	~ 80% (12-16w)	N/A	N/A	N/A
58	NPC	SD	3 $X10^5$	8,960 ± 3,029 (8w)	52.46% ± 6.28% (4-8w)	N/A	N/A	N/A
44	D28 (Corin sorted at D12)	SD	4$X10^5$	1687 ± 585 (16w)	~ 75% (12-16w)	N/A	N/A	N/A
59	D21	SD	1 $X10^5$	1,800 ± 1,506 (3w)	N/A	N/A	N/A	N/A
60	D16 (Corin sorted at D12)	X-SCID	N/A	N/A	~ 90% (16w)	N/A	N/A	N/A
45	D28 (LRTM1 sorted at D14)	SD	1.3$X10^5$	9002 ± 1,974 (16w)	~ 80% (12-16w)	N/A	N/A	N/A
61	D28 (Corin sorted at D12)	SD	4$X10^5$	56.8-65.5 (16w)	~ 65-90% (8-16w)	N/A	N/A	N/A
62	D16 (IAP sorted)	SD	1.5$X10^5$	~ 300 (6w)	N/A	N/A	N/A	N/A
63	D33 (cryo)	SD	4.5$X10^5$	5,796±446 (24w)	~ 100% (8-24w)	N/A	N/A	N/A

Abbreviations: CR, Charles River; cryo, cryopreserved cells; N/A, not available; NPC, neuronal precursor cells; SD, Sprague Dawley; X-SCID, X-linked severe combined immunodeficiency

* 2,106 ±313/mm^3 indicated DA density and DA yield result was not available in this study.

Supplemental Table 7. List of primer sequences used in this study

Gene	Full gene name	Sequences(fwd/rev)
EBNA #1 (EB-01)	Epstein-Barr virus-encoded nuclear antigen	5'-GAGAAAAGAGGCCCAGGAGT-3'
		5'-CCCCTACAGGGTGGAAAAAT-3'
EBNA #2 (EB-02)		5'-GGCAGTGGACCTCAAAGAAG-3'
		5'-CTATGTCTTGGCCCTGATCC-3'
EBNA #3 (EB-03)		5'-GGGTGATAACCATGGACGAGG-3'
		5'-ACTTGGACGTTTTTGGGGTC-3'
EBNA #4 (EB-04)		5'-ATAACCATGGACGAGGACGG-3'
		5'-GCAGCCAATGCAACTTGGAC-3'
EBNA #5 (EB-05)		5'-GGGTAGAGGACGTGAAAGAGC-3'
		5'-GGAGACCCGGATGATGATGAC-3'
D17S1290		5' CAACAGAGCAAGACTGTC 3'
		5' GGAAACAGTTAAATGGCCAA 3'
D7S796		5' TTTTGGTATTGGCCATCCTA 3'
		5' GAAAGGAACAGAGAGACAGGG 3'
D10S1214		5' ATTGCCCCAAAACTTTTTTG 3'
		5' TTGAAGACCAGTCTGGGAAG 3'
D21S2055		5'AACAGAACCAATAGGCTATCTATC 3'
		5' TACAGTAAATCACTTGGTAGGAGA 3'
ACTIN	Actin beta (ACTB)	5' CATGTACGTTGCTATCCAGGC 3'
		5' CTCCTTAATGTCACGCACGAT 3'
CORIN	Serine peptidase (CORIN)	5'-AATGGGAGTGAACCTTTGGTCA-3'
		5'-GTCGGGATGTGCAGTAGACA-3'
COL6A2	Collagen type VI alpha 2 chain	5'-TCATGAAACACGAAGCCTAC-3'
		5'-CACCCTTCTCTCCTTTGAAG-3'
CK8	Keratin 8 (KRT8)	5'-CCTGGAAGGGCTGACCGACGAGATCAA-3'
		5'-CTTCCCAGCCAGGCTCTGCAGCTCC-3'
DAT	Solute carrier family 6 member 3	5'-ACAGAGGGGAGGTGCGCCAGTTCACG-3'
		5'-ACGGGGTGGACCTCGCTGCACAGATC-3'
ECAT1	KH domain containing 3 like, subcortical maternal complex member (KHDC3L)	5'-CGAAGGTAGTTCGCCTTGAG-3'
		5'-CGGTGATAGTCAGCCAGGTT-3'
EN1	Engrailed-1	5'-CGTGGCTTACTCCCCATTTA-3'
		5'-TCTCGCTGTCTCTCCCTCTC-3'
ESRRB	Estrogen related receptor beta	5'-TGTCAAGCCATGATGGAAAA-3'
		5'-GGTGAGCCAGAGATGCTTTC-3'
FOXA2	Forkhead box A2	5'-GGTGCTTTGGCTGACTTTTT-3'
		5'-GTTGCTCACGGAGGAGTAGC-3'
GAPDH	Glyceraldehyde 3-phosphate dehydrogenase	5' ACCACAGTCCATGCCATCAC 3'
		5' TCCACCACCCTGTTGCTGTA 3'
GBX2	Gastrulation brain homeobox 2	5'-GGTGCAGGTGAAAATCTGGT-3'
		5'-GCTGCTGATGCTGACTTCTG-3'
GDF3	Growth differentiation factor 3	5'-AAATGTTTGTGTTGCGGTCA-3'
		5'-TCTGGCACAGGTGTCTTCAG-3'
GIRK2	Potassium voltage-gated channel subfamily J member 6	5'-GACCTGAAGTGGAGATTCAACC-3'
		5'-TGTATGCGATCAACCACCAGA-3'
GLI1	GLI family zinc finger 1	5'-GGGTGCCGGAAGTCATACTC-3'
		5'-GCTAGGATCTGTATAGCGTTTGG-3'
LMX1a	LIM homeobox transcription factor 1, alpha	5'-ACGGCCTAAAGATGGAGGAG-3'
		5'-CGGTAGAAGCAGGTGGTCTC-3'
MAP2	Microtubule associated protein 2	5'-CAGGTGGCGGACGTGTGAAAATTGAGAGTG-3'
		5'-CACGCTGGATCTGCCTGGGGACTGTG-3'
MSX1	MSH homeobox 1	5'-CGAGAGGACCCCGTGGATGCAGAG-3'
		5'-GGCGGCCATCTTCAGCTTCTCCAG-3'
MYL2A	Myosin light chain 7 (MYL7)	5'-GGGCCCCATCAACTTCACCGTCTTCC-3'
		5'-TGTAGTCGATGTTCCCCGCCAGGTCC-3'
NANOG	Nanog homeobox	5'-CAAAGGCAAACAACCCACTT-3'

		5'-TCTGCTGGAGGCTGAGGTAT-3'
NESTIN	Nestin	5'-TTGCCTGCTACCCTTGAGAC-3'
		5'-GGGCTCTGATCTCTGCATCTAC-3'
NKX2.1	NK2 homeobox 1	5'- CTCGCTCATTTGTTGGCGA-3'
		5'- GGAGTCGTGTGCTTTGGACT-3'
NKX2.2	NK2 homeobox 2	5'-CCGGGCCGAGAAAGGTATG-3'
		5'-CTGTAGGCAGAAAAGGGAA-3'
NURR1	Nuclear receptor subfamily 4, group A, member 2	5'-CACTCTTCGGGAGAATACAG-3'
		5'-CATTTGGTACAAGCAAGGTG-3'
OCT4	POU class 5 homeobox 1	5' GAAGGATGTGGTCCGAGTGT 3'
		5' GTGAAGTGAGGGCTCCCATA 3'
OTX2	Orthodenticle homeobox 2	5'-ACAAGTGGCCAATTCACTCC-3'
		5'-GAGGTGGACAAGGGATCTGA-3'
PAX6	Paired box 6	5'-ACCCATTATCCAGATGTGTTTGCCCGAG-3'
		5'-ATGGTGAAGCTGGGCATAGGCGGCAG-3'
PITX3	Paired like homeodomain 3	5'-GGAACCGCTACCCCGACATGAG-3'
		5'-TGAAGGCGAATGGAAAGGTCT-3'
REX1	ZFP42 zinc finger protein	5'-GGCGGAAATAGAACCTGTCA-3'
		5'-CTTCCAGGATGGGTTGAGAA-3'
SOX1	SRY-box 1	5'-CCTCCGTCCATCCTCTG-3'
		5'-AAGCATCAAACAACCTCAAG-3'
SOX2	SRY-box 2	5'-AACCCCAAGATGCACAACTC-3'
		5'-CGGGGCCGGTATTTATAATC-3'
SOX17	SRY-box 17	5'-CGCTTTCATGGTGTGGGCTAAGGACG-3'
		5'-TAGTTGGGGTGGTCCTGCATGTGCTG-3'
TH	Tyrosine hydroxylase	5'-CGGGCTTCTCGGACCAGGTGTA-3'
		5'-CTCCTCGGCGGTGTACTCCACA-3'
TUJ1	Tubulin beta 3 class III	5'-CGGTGGTGGAGCCCTACAAC-3'
		5'-AGGTGGTGACTCCGCTCAT-3'

Supplemental Table 8. List of Reagents or Resource used in this study

REAGENT or RESOURCE	SOURCE	IDENTIFIER
Antibodies		
Goat anti-ALDH1A1	R&D System	Cat.# AF5869
Rabbit anti-5-HT	Sigma-Aldrich	Cat.# S5545
Rabbit anti-Calbindin	Millipore	Cat.# AB1778
Rabbit anti-cleaved Caspase-3	Cell Signaling	Cat.# 9661
Rabbit anti-DARPP32	Abcam	Cat.# AB40801
Rabbit anti-DAT	Millipore	Cat.# AB5802
Mouse anti- Dopamine β Hydroxylase	Millipore	Cat.# MAB308
Mouse anti-FOXA2	Abnova	Cat.# H00003170-M10
Rabbit anti-GABA	Sigma-Aldrich	Cat.#A2052
Rabbit anti-GIRK2 (Kir3.2)	Alomone Labs	Cat.# APC-006
Mouse anti-NCAM(ERIC1)	Santa Cruz	Cat.# sc-106
Mouse anti-Synaptophysin	Thermo Fisher	Cat.# 14-6525-80
Rabbit anti-KI67	Abcam	Cat.# AB16667
Rabbit anti-LMX1A	Millipore	Cat.# AB10533
Rabbit anti-MAP2	Millipore	Cat.# AB5622
Mouse anti-NESTIN	Millipore	Cat.# MAB5326
Rabbit anti-NURR1	Sigma-Aldrich	Cat.#ABN1675
Mouse anti-PAX6	DSHB	Cat.# PAX6
Goat anti-SOX1	R&D System	Cat.# AF3369
Mouse anti-hNuc (STEM101)	Clontech	Cat.# Y40400
Rabbit anti-TH	Pel-Freez	Cat.# P40101-0
Sheep anti-TH	Millipore	Cat.# AB1542
Rabbit anti-TPH2	Novus Biologicals	Cat.# NB100-74555
Mouse anti-Tuj1	Biolegend	Cat.# MMS-435P
Mouse anti-TRA-1-60	Santa Cruz	Cat.# sc-21705
Rabbit anti-NANOG	Santa Cruz	Cat.# sc-33759
Mouse anti-SSEA-4	Millipore	Cat.# MAB4304
Mouse anti-OCT-4	Santa Cruz	Cat.# sc-5279
Rabbit anti-OCT-4	Cell Signaling	Cat.# 2750
Goat anti-OTX2	R&D System	AF1979
Rabbit anti-SOX2	Thermo Fisher	Cat.# 48-1400
Rabbit anti-SOX6	Abcam	Cat.# AB30455
Goat anti-OTX2	R&D System	AF1979
Goat anti-BRACHYURY	R&D System	AF2085
Goat anti-SOX17	R&D System	AF1924
Mouse anti-Vimentin	Dako	Cat.# M0725
Mouse anti-VMAT2	R&D System	Cat.# MAB8327

PE mouse anti-SSEA-4	BD	Cat.# 560128
PE mouse anti-TRA-1-60	BD	Cat.# 560193
Donkey F(ab')2 Anti-rabbit IgG H&L (Alexa Flour 488)	Abcam	Cat.# AB181346
Donkey F(ab')2 Anti-rabbit IgG H&L (Alexa Flour 568)	Abcam	Cat.# AB175694
Donkey F(ab')2 Anti-rabbit IgG H&L (Alexa Flour 647)	Abcam	Cat.# AB181347
Donkey F(ab')2 Anti-mouse IgG H&L (Alexa Flour 488)	Abcam	Cat.# AB150101
Donkey anti-mouse IgG H&L; Alexa Fluor 568	Abcam	Cat.# AB175699
Donkey F(ab')2 Anti-mouse IgG H&L (Alexa Flour 647)	Abcam	Cat.# AB150103
Donkey Anti-Sheep IgG H&L (Alexa Fluor 568)	Abcam	Cat.# AB175712
Donkey F(ab')2 Anti-goat IgG H&L (Alexa Flour 568)	Abcam	Cat.# AB175705
Chemicals, Peptides, and Recombinant Proteins		
DMEM	Thermo Fisher	Cat.# 11965092
DMEM/F-12	Thermo Fisher	Cat.# 11320033
mTeSR™-1	STEMCELL Technologies	Cat.# 85870
Essential 8 medium	Thermo Fisher	Cat.# A1517001
Fetal bovine serum (FBS)	Thermo Fisher	Cat.# 26140079
Knockout serum replacement (KSR)	Thermo Fisher	Cat.# 10828010
L-Glutamine	Thermo Fisher	Cat.# 25030081
Non-essential amino acids (NEAA)	Thermo Fisher	Cat.# 11140050
Sodium butyrate (NaB)	Sigma-Aldrich	Cat.# 303410
Nicotinamide (NAM)	Sigma-Aldrich	Cat.# N0636
0.5M EDTA solution	Thermo Fisher	Cat.# 15575020
Accutase	Millipore	Cat.# SCR005
TrypLE	Thermo Fisher	Cat.# 12605010
β-mercaptoethanol	Thermo Fisher	Cat.# 21985-023
N2 supplement	Thermo Fisher	Cat.# 17502048
CryoStor® CS10	BioLife Solutions	Cat.# 210102
SB431542	Cayman Chem	Cat.# 13031
LDN193189	Stemgent	Cat.# 04-0074
Purmorphamine	StemRD Inc.	Cat.# PUR-25
CHIR99021	Cayman Chem	Cat.# 13122
DAPT	Cayman Chem	Cat.# 13197
Boc-D-FMK	Cayman Chem	Cat.# 16118
Quercetin	Sigma-Aldrich	Cat.# Q4951
Y-27632	Selleckchem	Cat.# S1049

Ascorbic acid (AA)	Sigma-Aldrich	Cat.# A4403
dbcAMP	Sigma-Aldrich	Cat.# D0627
SHH	PeproTech	Cat.# 100-45
BDNF	PeproTech	Cat.# 450-02
GDNF	PeproTech	Cat.# 450-10
TGF-β3	R&D System	Cat.# 243B3010
FGF-8	PeproTech	Cat.# 100-25
Recombinant human FGF2 (bFGF)	Thermo Fisher	Cat.# PHG0023
Poly-L-ornithine solution	Sigma-Aldrich	Cat.# P4957
Fibronectin	Sigma-Aldrich	Cat.# F0895
Laminin	Sigma-Aldrich	Cat.# L2020
Matrigel matrix	Corning	Cat.# 354277
6-OHDA	Sigma-Aldrich	Cat.# H116
Desipramine	Sigma-Aldrich	Cat.# D3900
D-Amphetamine	Sigma-Aldrich	Cat.# A5880
Hoechst 33342	Thermo Fisher	Cat.# H3570
Trizol	Thermo Fisher	Cat.# 15596026
SuperScript® II Reverse Transcriptase	Thermo Fisher	Cat.# 18064-014
SsoAdv Univer SYBR SMX 5000	Bio-Rad	Cat.# 1725275
Tetrodotoxin	Tocris	Cat.# 1078
Picrotoxin	Millipore	Cat.# 528105
NBQX	Tocris	Cat.# 1044
D-AP5	Tocris	Cat.# 0106
PolyJet transfection reagent	SignaGen laboratories	Cat.# SL100688
Critical Commercial Assays		
Venor GeM Mycoplasma Detection Kit	Sigma-Aldrich	Cat.# MP0025
Neon transfection system	Thermo Fisher	Cat.# MPK1096
Bradford protein assay	Bio-Rad	Cat.# 5000201
GeneJET Plasmid Miniprep Kit	Thermo Fisher	Cat.# K0503
DNeasy Blood & Tissue Kit	QIAGEN	Cat.# 69504
QIAamp DNA FFPE Tissue Kit	QIAGEN	Cat.# 56404
Vectastain Elite ABC Kit	Vector Laboratories	Cat.# PK-6100
DAB peroxidase substrate Kit	Vector Laboratories	Cat.# SK-4100
Cell Mito Stress Test Kit	Agilent Technologies	Cat.# 103010-100
Cell Energy Phenotype Test Kit	Agilent Technologies	Cat.# 103275-100
Cell Lines		

Human BJ dermal fibroblasts	ATCC	CRL-2522
WA09 hESC cell line	WiCell Institute	WAe009-A
H7 hESC cell line	WiCell Institute	WAe007-A
iPS-DF19-9-11T	WiCell Institute	
Human adult fibroblasts	Coriell Institute	Cat.# GM03529
HEK293T cells	ATCC	CRL-11268
Recombinant DNA		
pGEM-T Easy vector	Promega	Cat.# A1360
pCXLE-EGFP episomal vector	Addgene	Cat.# 27082
FUW-tetO-MCS vector	Addgene	Cat.# 84008
FUW-tetO-hMYC	Addgene	Cat.# 20723
FUW-tetO- SOX2	Addgene	Cat.# 20724
FUW-tetO- KLF4	Addgene	Cat.# 20725
FUW-tetO- OCT4	Addgene	Cat.# 20726
STEMCCA lentiviral vector	Mostoslavsky's lab	
psPAX2	Addgene	Cat.# 12260
pMD2.G	Addgene	Cat.# 12259
Software and Algorithms		
Image J	National Institutes of Health	Version 2.0
Stereo Investigator	MBF Bioscience	Version 2017
Axion BioSystems's Neural Metric Tool	Axion Biosystems	Version 2.2
AxIS Navigator software	Axion Biosystems	Version 1.5.1
C6 software	BD Biosciences	
BWA-MEM	http://bio-bwa.sourceforge.net/	Version 0.7.15
SAM tools	https://samtools.github.io/	Version 1.3.1
Picard tools	https://broadinstitute.github.io/picard/	Version 2.5.0
Genome Analysis Toolkit MuTect2	https://software.broadinstitute.org/gatk	Version 3.6.0
Variant Effect Predictor	https://www.ensembl.org/vep	Version GRCh38.89 (annotation cache version 89)
ngCGH	https://github.com/seandavi/ngCGH	Version 0.4.4
Integrated Genome Viewer	http://software.broadinstitute.org/software/igv/	Version 2.3.79
Personalis Cancer Exome pipeline	Personalis, Inc., CA, USA	ACE3
R	The R foundation	Version 3.4